BADP-G's structural performance subjected to tsunami wave loading and its attenuated ground acceleration sourced from Manila Megathrust

By

MOHAMAD AFIQ BIN MOHD JUHARI

13516

Final Dissertation Report

Submitted to the Civil Engineering Programme
In Partial Fulfilment of the Requirements
For the Degree
Bachelor of Engineering (Hons)
(Civil Engineering)

AUGUST 2014

Supervised by : Associate Professor Ir. Dr. Mohd. Shahir Liew

Internal Examiner : Dr. Zubair Imam Syed

External : Ir Khairul Anwar Masud

Universiti Teknologi PETRONAS

Bandar Seri Iskandar

31750 Tronoh

Perak Darul Ridzuan

CERTIFICATION OF APPROVAL

BADP-G's structural performance subjected to tsunami wave loading and its attenuated ground acceleration sourced from Manila Megathrust

By

Mohamad Afiq bin Mohd Juhari

A project dissertation submitted to the

Civil Engineering Programme

Universiti Teknologi PETRONAS

in partial fulfilment of the requirement for the

BACHELOR OF ENGINEERING (Hons.)

CIVIL ENGINEERING

Approved by,

____

(Assoc. Prof. Ir. Dr. Mohd Shahir Liew)

Universiti Teknologi PETRONAS

Bandar Seri Iskandar

31750 Tronoh

Perak Darul Ridzuan

MAY 2013

CERTIFICATION OF ORIGINALITY

This is to certify that I am responsible to the work submitted in this project, that the original work is my own except as specified in the references and acknowledgements, and that the original work contained herein have not been undertaken or done by unspecified sources and person.

(Mohamad Afiq bin Mohd Juhari)

Abstract

The main approach of this paper is paper is to study the effect of a natural phenomenon known as tsunami waves and its attenuated seismic ground loading in Sarawakian water sourced from Manila Trench which situated for almost 1200km away from BADP-G platform. General practice is the design of fixed offshore platforms in Malaysia are governed primarily by the wave forces at the sea. However, seismic analysis is not taken into the design consideration simply because Malaysia's location is situated on a stable Eurasian plate in the sense of having very low seismic activity. There is, hence, a need to assess this platform when the platform is actually seen to be exposed to a tsunami threat in the north-east of Malaysia at the Manila Trench. The project shall envelope a simulation approach of regenerating the tsunami wave properties based on vital geological parameters of the Manila Trench. As the trench ruptures, tsunami wave is formed and followed by lateral ground movement of the earth. Calculation of the attenuated lateral ground movement produced from the rupture is calculated through an equation to predict the peak ground acceleration of a given distance in South China Sea region. The project shall continue in finding the most severe direction by applying omni-directional 100 years storm wave as per designed and the maximum joint displacement of that direction shall be picked as the worst direction. Primarily, the main body of the project is ascertaining the tsunami wave height plus its attenuated ground acceleration will induced the failure of the platform's leg through member maximum unity check and joint displacement coming from the worst direction of force is analyze by using a finite element software known as SACS 5.3. For each scenario, the input of tsunami wave height is increased and analyzed by using static analysis with non-linear pile interaction; of which the static behavior of the platform will be then investigated. As expected, a threshold of a tsunami wave height is obtained at a point where the platform leg fails. Ultimately, the annual rate of exceedence is then predicted through return period of the threshold tsunami wave height that leads to the failure of the BADP-G platform.

ACKNOWLEDGMENT

بِسۡمِ ٱللَّهِ ٱلرَّحۡمَٰنِ ٱلرَّحِيمِ

In the name of Allah, The Beneficent, The Merciful

First and foremost the author would like to praise Allah the Almighty for His blessings and bestow-ness upon completing the final dissertation report. What could be worse than without the support from Him, our lord to where only Him we will serve and prostrate and to where only Him we belong.

Special thanks to AP Ir. Dr. Shahir Liew who are very pleasing in giving out informational and educational approach to the author. He is very supportive and responsive to any uncertainty that the author faced in the epoch of the on-going work and research that had been done lately.

Heartfelt appreciation is given to the Mr. David Flock for his never-ending hard work to deliver his knowledge and skills to help the author solve problem along the way. He is known to have so many unattended jobs but still very supportive to help the author. The gratitude goes on for the rest of the UTP OECU's team for their guidance in getting vital information upon the structural parameters and explanation from the beginning of the final year project until the end.

TABLE OF CONTENTS

CHAPTER 3 : METHODOLOGY AND PROGRESS

CHAPTER 4 : RESULTS

CHAPTER 5 : CONCLUSION

LIST OF FIGURES

LIST OF TABLES

Chapter 1

1. Introduction

Malaysia's economic growth is driven by the oil and gas exploration and production because the abundance of oil supply on their seas. To extract the oil, offshore platform are required for drilling, production and accommodations of the personnel purposes. Significantly, these offshore platforms are constantly being loaded by metocean loadings; wave, wind and current specifically because Malaysia is believed to be unassailable against lateral seismic loading since it is situated on a stable Eurasian plate. However, far field earthquakes have been felt on rare cases around the country sourced from neighboring country such as Indonesia and Philippines. Reminiscing from the year 2004, Acheh was slammed by an earthquake of M_w = 9.3 and the effect was relatively disastrous as it results to a giant tsunami that killed hundreds of thousands of Indonesians, 68 of Malaysian residents were apparently killed and surprisingly the tsunami even travelled thousands of kilometers away to the Eastern Coast of Africa including Tanzania, Kenya and the isle of Madagascar. Eventhough this disastrous effect will be more severe on the shore compared to offshore, there are no discount on possibilities of platform's survivability around Sarawak water to survive after it is hit by the loadings.

Furthermore, envisage another active sub-continental crust rupture against another oceanic crust at the Manila Trench which has the potential to recur as the Andaman Trench, Acheh which might wipe away the offshore platform if it is to happen. Thus, PETRONAS must anticipate this problem from jeopardizing the oil and gas business in Malaysia. In the recent days, it is understood and accepted by the top management to not considering any seismic and tsunami risks to the oil platform since the potential source of seaquakes are just far off to be a hazard to the platform. However, studies had convinced the experts to start to take this problem more serious as it is believed to be a potential threat to their assets around Sarawakian waters.

1.1 Problem Statement.

Almost all the offshore platform residing in Malaysia are confined to the standard code of design as what PTS standards being used. Offshore platform designs are limited; where seismic loading is not taken into consideration previously because it is assumed that Malaysia is in the low risk zone of receiving seismic activity. This paper is focused on one potential source of seaquake which is from the Manila Trench or known as Manila Megathrust; situated North-east of Malaysia with a distance of almost 1200km away. It is believed that when the Megathrust rupture soon, a big tsunami and a slight ground acceleration will be felt around Sarawakian waters.

For that, BADP-G, a drilling platform will be representing all platform around the Baram Field, Sarawak. The chosen platform will be tested with two pre-eminent loadings which are ground acceleration that is produced from the intensity of the seaquake by moment magnitude (mw) and the resultant tsunami wave loading that is produced from the seaquake. Thus, a comprehensive study will be done to ascertain the threshold intensity of the seaquake by moment magnitude will actually results to the maximum lateral ground acceleration plus with the tsunami wave loading the platform can withstand before the structure fail.

1.2 Objectives

1. The **primary objective** of this study is to perform a computer-based simulation on the structural response of the BADP-G, a four legged jacket platform subjected to lateral ground acceleration, tsunami wave loads and PCSB operational metocean loads.

Each of every earthquake's moment magnitude will results to different tsunami wave height, wave period and different lateral ground acceleration. By using TUNA-M2 software, the tsunami wave loading is simulated and then plotted into graph and the maximum wave height and period is recorded for that particular wave profile.

Then, the attenuation of the ground acceleration from the seaquake is calculated by hand using a formula suggested by (AULOV & LIEW) of where both of them had developed Malaysia-specific ground motion prediction equation for all earthquake sources.

Lastly, by using SACS 5.3 software, the structure is simulated by subjecting it with the calculated attenuated ground acceleration, tsunami wave loading (generated from TUNA-M2 of the maximum height and period of the wave) and the metocean data under operational condition. (As per PTS).

2. The **secondary objective** of this study is to determine BADP-G's structural integrity by defining the point where the structure fails.

Corresponding to the loading that the structure will face in every increment of the seaquake intensity, the robustness of the platform is checked for every seaquake's intensity increment to actually address to what failure mechanism will lead to the failure of the platform.

1.3 Scope of study

BADP-G is taken to represent the whole fleet of Baram Field because of the nature of the design to be of one of the shallowest platform in Sarawakian waters. With this, wave shoaling effect will be greater as the tsunami wave height will increase in height as the depth of the water decreases. Thus, the increase of tsunami wave height will further increase the risk of the platform from collapsing thus the latter assumption is seemingly justified.

The structural model that was obtained from PCSB is not complete beforehand, and thus the model is made available by reassigning missing members from the model by looking at the design reports and to make sure that the scope of analysis of the report will cover to the nearest approximation of the actual behavioral of the platform. In addition, a complete set of data of the design reports was available, thus, the author chose this platform to perform the study.

Chapter 2

Literature Review and Theory

2. Manila Trench seismicity

In the recent study, it is proved that Manila Trench is seismically active as the tectonic plates on the subduction zone are still moving (Kreemer, Holt, Goes, & Govers, 2000; Megawati et al., 2009; Ruangrassamee & Saelem, 2009). From a measurement based on a GPS geodesy, the convergence rate on the trench is about 8-9cm/year (Megawati et al., 2009). At any point of time, the plates stresses has to be accommodated and the results of the tsunami is estimated to range from 8.0 Mw – 9.0Mw but there are no guarantee that the earthquake intensity will be at that range. This is because by comparison from previous events, 2004 Andaman Tsunami's coseismic slip is between 12-15 meters results to 9.3 ritcher scale while the megathrust is noted to have a maximum of 40 meter slip on the median part of the trench.(Dao, Tkalich, Chan, & Megawati, 2009; Koh, Teh, Liu, Ismail, & Lee, 2009).

To predict Manila Trench true potential as a far-field seismic and tsunami threat to the offshore platform, a comparison is made with the Andaman Trench which recently ruptured in 2004 with a moment magnitude of 9.3. Both of the trenches have more or less the same characteristic; a Megathrust of two plates grinding each other and the denser crust is subducting into the other, depth is less than 70km which categorized them as a shallow subducting earthquake, both of them are proven to be active and still moving accumulating stress on the subduction zone, and both can be considered far-field earthquake by the distance from the focus of the subduction stress and the offshore structure.

The United States of Geological Survey (USGS), Earthquake Hazards Program had already studied the problem thoroughly and approximated that the zone of faulting is almost 1300km long. Studies also shown that the northern part of the fault zone is contributing to the primary shock fault rupture of almost 500km away. Due to the shock, it may trigger the vicinity faulting around the primary shock zone but however, there is no proven fact that the faulting correspond to a single slip of the each fault nor to remote activity from the primary shock rupturing. It is suggested that also the width of the faulting is nearly more than 150 and the maximum dislocation distance on the fault plane is 20 meters. All this parameters above play role in determining the resultant moment magnitude of each earthquake.

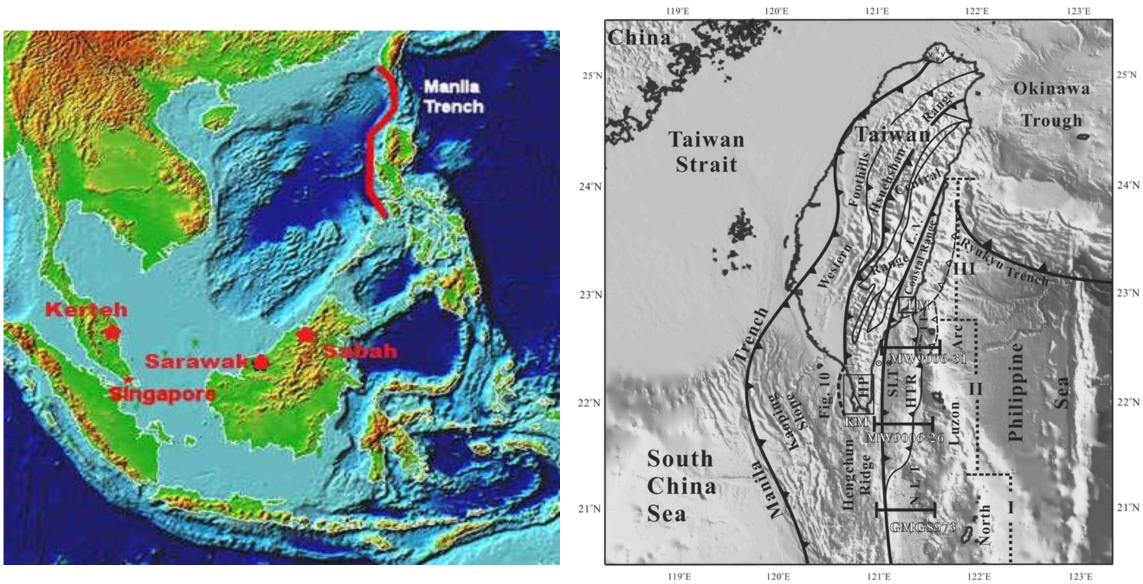

Figure 1: Study Area (Left) and close up illustration of Manila Trench (right)

To compare with the recent Andaman Trench with the Manila Trench, several authors had giving results on their respective papers. The summary of the geological features are represented on a table 1 below.

Geological Characteristic	**Andaman Trench (2004) (Mw = 9.3)**	**Manila Trench (Soon) (Mw =?)**
Length of fault	1300km (USGS)	• **980 km** (Wang, X. and Liu, P, L, F.) • **990 km** (Huang et al., 2009) • **1000km** (Dao et al., 2009)
Width	150km (USGS)	• **200km** (Wu & Huang, 2009) • **150km maximum** (Dao et al., 2009)
Coseismic Slip	20m (USGS)	• **20m** (Wu & Huang, 2009)

		• Lowest **5m** & Highest **40m** (Dao et al., 2009; Megawati et al., 2009)

Table 1: Geological Aspect comparison between Andaman and Manila Trench

After all this comparison, ultimately we wanted to have an idea of what is the intensity by moment magnitude of the earthquake does this Manila Trench potentially to be? Based on the parameters above, we could predict that the geological parameters of the Manila Trench compared to Andaman trench is nearly similar and expect that the intensity of the earthquake to be somewhere around 8.5Mw-9.5Mw; somewhere in that range. However, the tsunami it can generated and the intensity of the earthquake lies on many other factor as well. As to complement the latter, it seems to be fairly justified.

This is supported by (Dao et al., 2009; Huang et al., 2009) where based on their study they simulated the worst case tsunami threat in the South China Sea would be at 9Mw or greater which is quite as same as the Andaman Trench.

2.1 Plate tectonic theory

Seismic waves are energy waves that is generated from rock breaking within the earth and usually comes with an explosion. The explosion is usually driven by the sliding between two plate tectonics which grind each other on a fault surface and develop stress at that surface. Earth’s mantle; a layer of hot molten dense rocks under the crust is responsible for the movement of the plate tectonic as it creates convection current movement under the earth’s crust making the plates moves around and creates tectonic boundaries. There are three types of tectonic boundaries which are convergent boundaries, divergent boundaries and transform boundaries. Basically, convergent boundaries happen when the plates collided converging towards each other creating mountain ridges and trenches; Mountain ridges happens if collision between two continental plates and oceanic trenches formed when two plates converging in the ocean for one of the plates is subducting towards inside the earth. Divergent boundaries happen when two plates diverge away from each other creating new ridges and meanwhile transformation boundary happen when two plates which slide sideways past each other.

Manila Trench is classified as a Megathrust or by convergent boundaries from two plates from the Eurasian plates subducting towards the Philippine plate as shown in figure 2 below.

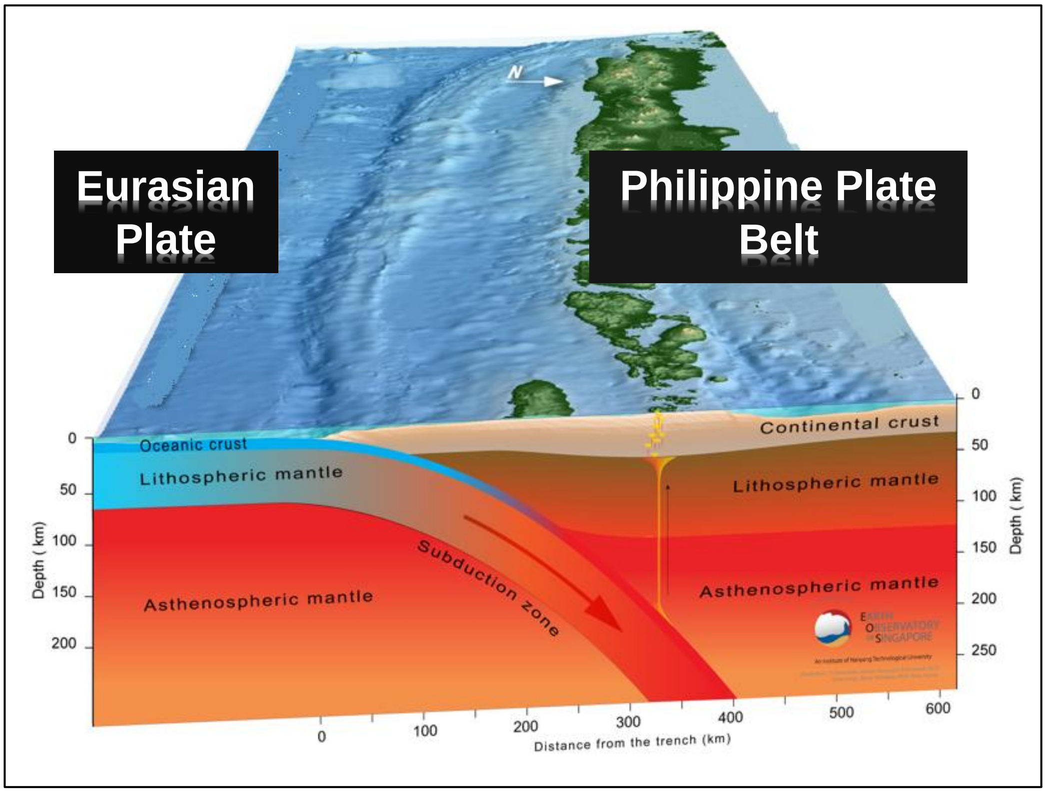

Figure 2: Cross Section of the Manila Trench

2.2 Seismic Waves

Seismic wave can be divided into two which are body waves and surface waves. Body waves propagates through solid and liquid medium within the earth and surface waves can only propagate across the surface of the earth's crust only.

Body waves have two types of waves which are Primary Waves (P-wave); longitudinal or compressional waves which travel the fastest between all the waves, and Secondary Waves (S-Waves) ; traversing or shearing wave that moves horizontal side-to-side motion or vertical up-and-down which then introduces shear stress along the rock of where the waves propagates. Plus, the natural characteristic of the waves are analogous with longer period with large amplitude inhibit it from travelling into fluidal or gaseous medium (Elnashai & Di Sarno, 2008). The average speed of the compressional wave is in the range of 1.5 - 8 kilometer per hour (kph) while traversing wave travels more than halves of the speed of P-Waves depending upon the density of the rock it travels.

Surface waves travel rather much slower than body wave but it mainly contribute most of the destruction on the earth surface. These waves are generated from constructive interference of body waves which travelling parallel to the ground surface and various underlying boundaries(Elnashai & Di Sarno, 2008). There are two types of surface waves which are Rayleigh and Love Waves. Most of the shaking is felt from the propagation of Rayleigh waves however, love wave travel much faster compared to Rayleigh waves. Love waves or LQ are horizontally polarized surface waves and the wave propagates side-to-side on the earth's surface. The natural movement of Rayleigh wave rolls along the earth particle just like wave rolls across an ocean (Michigan Tech).

In terms of the properties of both of these waves, under Snell's law of refraction, both compressing and shearing waves can be reflected and refracted under the different layers of rock density. The amplitude of these waves will decrease linearly with the increase of the distance of X, while the amplitude of surface waves will attenuate inversely proportional to the square root of distance X. In addition, the influence of the energy released by the earthquake are governed by the amplitude and the period of this waves.(Elnashai & Di Sarno, 2008). Supposedly, the higher the amplitude and period of the wave will results to a higher intensity of the earthquake.

Magnitude is a quantitative approach to measure how intense the ground movement is based on the earth's geological fault dimensions. Recently, M_L (Ritcher) is used to measure the highest amplitude of the seismic wave by using standard Wood-Anderson seismographs. The natural period of the seismograph is recorded by 0.8 seconds and it is capable to amplify wave period between 0.5-1.5seconds and wavelengths of 500m up to 2000m. However, ritcher scale has limitation as it is applicable only for small earthquakes with Epicentral distances of less than 600km. Moreover, the scale is meant to read seismic waves in localize region (can be used only in California, USA) compared to other scale for example m_b, M_s and M_w are widely accepted scales around the world.(Elnashai & Di Sarno, 2008). As it can only estimate accurately the magnitude of the earthquake up to 6.5 ritcher scale, but beyond that the scale progressively underestimates the actual energy released by the rupture of the earthquake.(McCalpin, 1996)

Body wave magnitude (m_b) is develop years later when it purposes is to measure the P-wave's amplitude under the period of 1 seconds which have less than 10kilometers wavelengths. However, this scale is highly suitable to measure deep earthquake depths because compressional waves does not affect the depth source of energy. Plus, it can be used for Epicentral distance up to more than 1000km.(Elnashai & Di Sarno, 2008)

Surface wave magnitude (M_s) is to measure the amplitude of the LR waves (love waves) with a period of 20 seconds and wavelengths up to 60kilometers (common distances for earthquake). It can also tolerate Epicentral distances up to 2000km away from epicenter to the receiver. The limitation of the scale type it cannot be used under deep earthquakes as like the body wave scale can do.(Elnashai & Di Sarno, 2008)

Ultimately, the best scale that can be applied to measure the intensity of the earthquake is by using moment magnitude (M_w). By far, this is the most recent and widely used scale and fundamentally differs from the earlier scales. (Kanamori, 1983)The unique of this scale lies on shearing that take place on the earthquake sources and it is not related to any wavelength of the seismic wave. Thus, M_w can be used to measure the whole spectrum of ground motion and it is defined to be a function of the seismic moment, M_o (Elnashai & Di Sarno, 2008). The formula is shown as below.

$$Mo = D\ A\ \mu$$

Where D is the average displacement or slip distance of the entire fault surface, A is the area of the fault rupture and μ is the shear rigidity (modulus) of the crustal rock in the vicinity area of the fault. Usually, μ is taken as 3.0-3.5 x 10^{11} dyne/cm^2 for continental crust . Then, the moment magnitude is calculated by using the formula below.

$$Mw = \frac{2}{3}\log(Mo) - 10.7$$

Formula taken from (Papazachos, Scordilis, Panagiotopoulos, Papazachos, & Karakaisis, 2004)

Thus, moment magnitude is the most suitable scale that will be used in the study because it is applicable for all earthquake size; be it in small regional sized or the larger size, can tolerate to any earthquake depths without any limitation of the Epicentral distance. It relies only on the seismic moment which reflecting the actual geological parameters of the faults and it is accepted worldwide as to prove the point made by Kanamori (1977).

2.3 Tsunami waves

Tsunami waves is different compared to normal operating waves in the ocean whereby mostly the waves is basically wind-driven. Not only that, tsunami waves are characterized as series of shallow water waves with long wavelength and periods which possesses long wavelengths up to 100km away with a period over an hour. (Earth and Space Sciences, University of Washington). Majority of tsunami wave generation is generated from underwater earthquake or also known as seaquakes (impulsive underwater explosion). However, flank failure due to slope instability or volcanic eruption activity might have the potential to trigger tsunami waves.(Lehfeldt, Milbradt, Pluss, & Schuttrumpf, 2007)

Shallow water waves is classified by taking the ratio of depth against the wavelength which results of less than 0.05 or 1/20. (Water depth, d/ wavelength, L < 0.05). (Chakrabarti, 2005). Since tsunamis are typically shallow-water waves, they are governed by shallow-water wave equation. In using SACS software, there are no guarantee that the software would actually reflect the actual behavior of tsunami wave loading. However, the best way to simulate the real phenomenon is by treating the tsunami wave loading by Solitary Waves theory (via interview Prof. Kurian V. John, Expert in Offshore Structures).

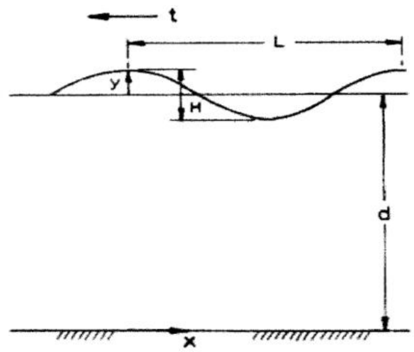

Figure 3: A flat bottom surface of a 2-dimensional wave motion

Water waves are excellent in carrying energy, transmitting energy from wind usually. In tsunamis case, the energy releases from the rupture is dissipated to the particle of the waters and thus disturbs the ocean's surface, a huge volume of water is displaced creating wave. Its speed may reach up to 800km/hour at a deeper water but the speed decreases as the wave approaches shore. Not only that, the wavelength will also decreases thus forcing the energy per unit are of the wave to concentrated as the area is decreasing as the depth of water is decreasing. The effect of that is the tsunami's wave height will slowly to increase as to contain the constant energy flux at a shallower water depth. However, at this point of time, the period of the wave is constant and does not change as the wave approaches the shore. After sometime, too much of wave height gain decreases the stability of the wave results to water breaking; an event where water curls forward and breaks. Typically, this happens when the height of the tsunami wave is almost the same as the local water depth. This is what we called as water-shoaling.

2.4 Fixed Jacket offshore platform (BADP-G)

Fixed offshore platform is a type of an offshore oil platform that is simply supported by steel jacket structure which is constructed at fabrication site before it is upended and launched into the sea. Typically, they are tubular-shaped and held by trusses to support the rigidity of the jacket structure. Highlighted by Chakrabarti(2005), bottom-founded structure is called as fixed because when their lowest natural frequency of flexural motion is above the highest frequency of significant wave excitation. The structure behave more as a unit of a body that need to resist dynamic metocean loading of the environment. Figure 4 is to show a typical jacket of an offshore platform. The jacket legs is made tubular in shape to resist the drag forces on the legs. Not only that, the inside diameter is kept hollow to slot in piles. In the event of installation of this structure, piles are inserted into the hollow slot on the jacket legs then acts as a guide to drive the pile all the way down to the seabed.

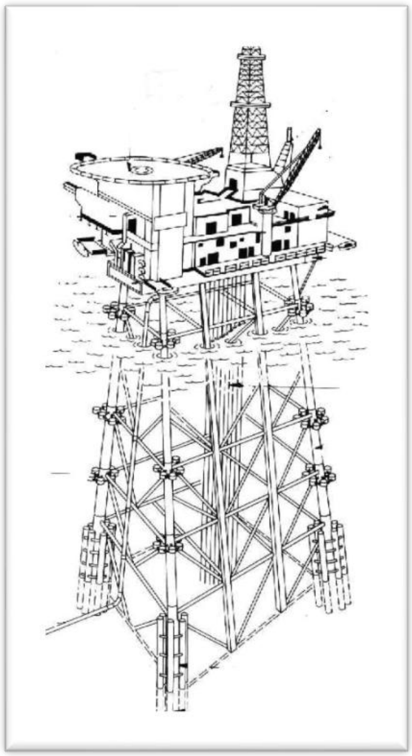

Figure 4: Typical Offshore Jacket Structure.

Depending upon the design on the spatial area of the site, a fixed jacket platform may have four up to eight legs to achieve stability against waves to prevent it from toppling over. There are many functional classification of an offshore oil gas platforms. One of the classification is wellhead platform where drilling activity and wellhead equipment is used on the topsides. It is to support very few equipment such as wellhead control panel and piping. Certain platform might also allow helipads; supported for helicopter landing purposes during emergency evacuations. Process platforms are used for production facilities and it is used to support in addition to equipment for production such as power generations, utilities and etc. Riser platform is used to support all incoming riser and outgoing riser on a planned complex. Sometimes, bridges are used to connect the main platform to the riser platforms. The living quarters platform is another function platform to support the personnel on the platforms. As a HSE practice, usually the living quarter is placed faraway from any danger exposure (far from processing platform) which has the potential to explode and protected by reinforced walls.

2.5 Standard and Code of practices used.

For any offshore platforms own by PETRONAS, the standard code that is used widely for the design of the structure is by following the PETRONAS Technical Standard (PTS 34.19.10.30), Revision 7, working stress design. In the document explains the requirements of the superstructure and substructure design, to detailing design of the joints, beam to beam connections, metocean loadings that is need to be considered and whole lot of list to be covered. However, seismic requirement is not included inside the PTS because generally, Malaysia is considered in the low seismicity area of where seismic activity is rarely to happen (seismic of zone 1 &2)(API, 2000). Thus, since PTS main reference is based on the American Petroleum Institute (API RP 2A WSD), Working Stress Design, any code, guidelines of the design requirement regarding seismic is referred to this document (API RP 2A WSD).

2.6 Structural Response towards seismic waves.

In the book of fundamental of earthquake engineering by (Elnashai & Di Sarno, 2008), there are three response characteristic that govern the behavioral of the structure and its foundation are the structural strength, ductility and stiffness. But, in API under section C2.3.6c and C2.3.6d, for seismic consideration purposes, it is enough to only consider the strength and ductility requirements of the structure.

Strength is the capacity of the structure to resist the load and to endure the deformation or deformation capacity and ductility is the ability of a group of components or structure’s to deform beyond its elastic limit.

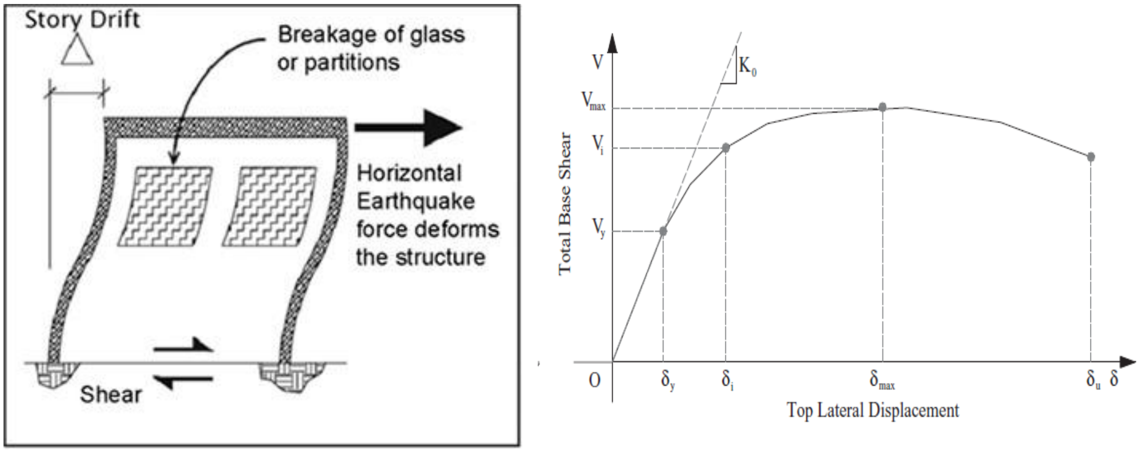

Figure 5: Definition of strength

In the figure 5 above, shows the behavior of a body when it is subjected with horizontal seismic force on proportional to the weight of the structure and it fixed member. It behaves more like a pendulum, the weight at the top of the structure acts as a counter weight and when the pendulum swings, it creates tension at the string of where the pendulum is tied. The further away the string from the pendulum, the higher the stresses will be. The results of the lateral forces is the base shear at the bases of the structure. In offshore structure, the greater the height of the platform, the higher the natural period of the structure will be, the higher the base shear it results to (Searer & Freeman, 2004). An adequate axial, flexural, and shear capacity is needed to withstand the base shear forces created by the lateral ground movement. Should any of the capacity fail to withstand the stresses, there is a chance of member failure and not limited to the global failure. Thus, it is important to check for the base shear in seismic concern.

Meanwhile, ductility is an important feature for offshore structure as it possess the ability to withstand more loading without entering to any plasticity stage. In this case, the performance of the structure is relying on the inelastic properties of the structure of where the structure has passed through elastic phase. This gives the more flexibility in terms of designing the structure economically without supersized section of the tubular members and whatnot. Figure 6 shows structural ductility after the structure is being loaded after sometime, with enough ductile requirements, the structure can still endure large lateral displacement with a slight reduce of the total base shear.

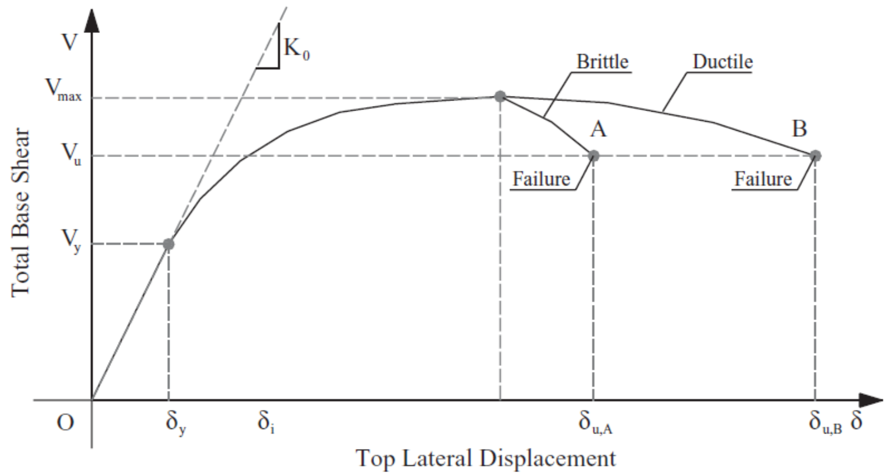

Figure 6: Definition of structural ductility

2.7 Ultimate Strength analysis.

It is stated in the API RP 2A WSD in 17.7.3 Ultimate Strength Analysis Procedure is to demonstrate the structural competency in its strength and stability to survive the ultimate strength loading. It is allowed to use linear global analysis first to determine of which members or joints will exceed the yielding and buckling strength. If a few of the localize members or joins exceeded its yielding strength, then local overload consideration will be put instead, otherwise, detailed global inelastic analysis is required. (API, 2000)

As prescribed in C17.7.3c.2, pushover analysis and time-domain analysis are accepted as to analyze the structure by non-linear collapse analysis (API, 2000). The main results of such analysis is the Reserve Strength Ratio (RSR) (Kheiri & Bahaari).

2.8 Reserve Strength Ratio (RSR)

The reserve strength ratio (RSR) is the ratio of ultimate collapse capacity of the structure against the design load for the structure. Similarly, a parameter that gives the ratio of collapse capacity of a damaged structure against the design load. Typically, the calculation of the RSR is held by an annual probability of exceedence of 100 years return period (PTS, 2012). Thus, the residual strength factor (RIF) is defined as the ratio of DSR against the RSR. RIF is a measure of the effect of the RSR when a member is damaged or loss. (Ersdal, 2005). The formula of RSR, DSR and RIF are shown as below.

$$RSR = \frac{Qu}{Qd} \quad , \qquad DSR = \frac{Qr}{Qd}$$

$$RIF = \frac{DSR}{RSR} = \frac{Qr}{Qu}$$

Where Qu is the ultimate load capacity, Qd is the design load of the structure, Qr, is true ultimate load capacity under damaged conditions. Figure shows that the illustration of the ultimate load capacity against deflection curve of a jacket structure with indication of the design load level and collapse load level in intact or damaged condition.

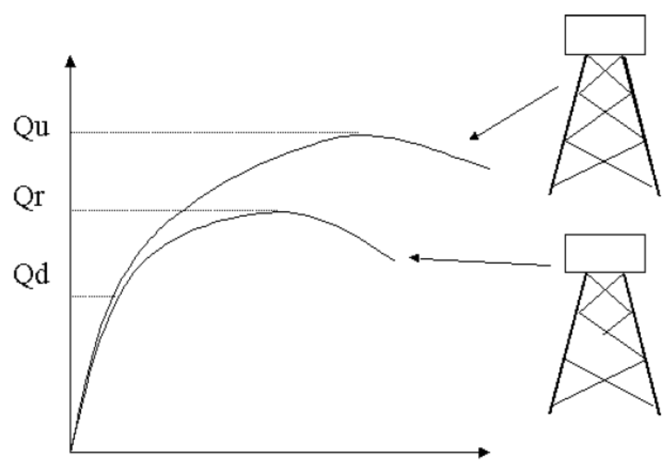

Figure 7: Illustration of the Q (ultimate capacity loading) against the deformation δ

2.9 Baram Drilling Platform (BADP-G) design data

BADP-G is a four-legged drilling platform. The structure was installed in 1994 in the Baram field standing tall at the height of 15m water depth from the seabed. All the main and skirt piles are 60-inch OD shimmed at the jacket structure. In the previous static inplace analysis report by Technic Coflexip in the year of 2002, The total jacket plus the topside load is equal to 1766 millions tonnes. Figure 8 shows a vintage picture of BADP-G and the summary of the Characteristic and design data are shown in the table 2 below.

Figure 8: A Vintage picture of Drilling Platform BADP-G

Characteristic and Design Data for BADP-G (taken from SICS (April, 2014)

Platform Design Data	Details
Platform Name	BADP-G
Field	Baram
Platform Type	Fixed Steel Jacket
Platform Function	Drilling
Heritage	PETRONAS
Installation Method	Lifting
Year Installed	1994
Design Engineer	Protek
Longitudinal Framing	X
Traverse Framing	X
Manned	No
Number of Bays	1
Number of Legs	4
Number of Piles	8
Number of Leg Piles	4
Number of Skirt Piles	4
Maximum Leg Diameter	1664mm
Grouted Piles	No
Jacket Weight (Generic)	629T
Deck Weight (Generic)	962T
Maximum Crane Size	2T
Helipad	Yes
Boat Landing	Yes

Shore Distance	27km
Water Depth	15.5 m
Design Air Gap	6.28 m
Design Deck Elevation	11.80 m
Design Code	API
Design Life	25 years
Design Return Period	100 years
Design Wave Height	7.7m
Design Current Speed	175 cm/s
Design Tide	0.9m
Design Caisson	2
Design Conductor	15
Design Riser	3
Design Marine Growth	152.40mm
Design Scour	1.5m
Design Deck Weight	962 T
Design Conductor Subsidence	38.1mm

Table 2: Characteristic and Design data of BADP-G

Chapter 3

3. Methodology

To perform the study, various steps will be carefully outlined in the current paper to represent the overall activity of the analyses required. In the report, the author have outline three key milestones for each main activity on finding the sources and any analyses that will be carried

- Gather relevant information from journal papers, books and online article.
- Meeting with experts (Prof Kurian, Doctor Shahir, Doctor AP Mus, Doc Berihun (geology aspect)

- Load analyzation (Flow Chart in the slide)

- Check BADP-G platform integrity
Find critical members that cause failure

out in the study. The three key milestones are represented in figure 9 as below:

Figure 9: Key Milestone of the Study

The definition of input gathering is more or less to research work on finding the related sources, finding best approach to solve the problem and asking experts opinions on how to actually “replicate” the best scenario to reflect the actual cause of the problem. In here, we are looking on three inputs that is strictly dependent upon the intensity by moment magnitude of the seaquake which are input for simulating the tsunami waves, input for seismic analysis and input for operating wave condition as per PTS suggest.

3.1 Input Gathering (TUNA-M2)

To simulate the tsunami waves, a set of geological data is needed to perform each and every set of seaquake intensity to produce the tsunami waves. Below is the set of data which are needed to generate 4 tsunami wave loads from Mw of 7 up to 9.2 which was suggested by Papazachos et al. (2004). The fault lines are divided by four segments and the length, the strike angle (o), dip, and rake are kept constant. The depth of the trench is marked with 40km length (given by USGS) and the width and co-seismic slip have been recalculate as it is necessary to do so because co-seismic at that depth is not expected. (CRUZ SALCEDO, 2011).

The below are all the input parameters to produce each of the tsunami waves.

Source	location of the fault		Length(km)	Depth (km)	Width(km)	Strike (°)	Dip	Rake(o)	Slip (cm)
	Longitude	Latitude							
1.00	120.00	20.00	277.00	40.00	166.72	20.00	41.00	79.00	1282.33
2.00	119.51	17.20	254.00	40.00	166.72	1.00	36.00	95.00	
3.00	119.46	15.00	238.00	40.00	166.72	359.00	40.00	98.00	
4.00	120.65	12.85	210.00	40.00	166.72	310.00	25.00	90.00	

Mw = 9.2

Source	Corner location of the fault		Length(km)	Depth (km)	Width(km)	Strike (°)	Dip	Rake(o)	Slip (cm)
	Longitude	Latitude							

1.00	120.00	20.00	277.00	40.00	144.54	20.00	41.00	79.00	954.99
2.00	119.51	17.20	254.00	40.00	144.54	1.00	36.00	95.00	
3.00	119.46	15.00	238.00	40.00	144.54	359.00	40.00	98.00	
4.00	120.65	12.85	190.00	40.00	144.54	310.00	25.00	90.00	

Mw = 9.0

Source	Corner location of the fault		Length(km)	Depth(km)	Width(km)	Strike (^{o})	Dip	Rake(o)	Slip (cm)
	Longitude	Latitude							
1.00	120.00	20.00	277.00	40.00	101.16	20.00	41.00	79.00	457.09
2.00	119.51	17.20	254.00	40.00	101.16	1.00	36.00	95.00	
3.00	119.46	15.00	238.00	40.00	101.16	359.00	40.00	98.00	
4.00	120.65	12.85	190.00	40.00	101.16	310.00	25.00	90.00	

Mw = 8.5

Source	Corner location of the fault		Length(km)	Depth (km)	Width(km)	Strike (^{o})	Dip	Rake(o)	Slip (cm)
	Longitude	Latitude							
1.00	120.00	20.00	277.00	40.00	70.79	20.00	41.00	79.00	218.78
2.00	119.51	17.20	254.00	40.00	70.79	1.00	36.00	95.00	
3.00	119.46	15.00	238.00	40.00	70.79	359.00	40.00	98.00	
4.00	120.65	12.85	190.00	40.00	70.79	310.00	25.00	90.00	

Mw = 8.0

Source	Corner location of the fault		Length(km)	Depth (km)	Width(km)	Strike (^{o})	Dip	Rake(o)	Slip (cm)
	Longitude	Latitude							
1.00	120.00	20.00	277.00	40.00	49.55	20.00	41.00	79.00	104.71
2.00	119.51	17.20	254.00	40.00	49.55	1.00	36.00	95.00	
3.00	119.46	15.00	238.00	40.00	49.55	359.00	40.00	98.00	
4.00	120.65	12.85	190.00	40.00	49.55	310.00	25.00	90.00	

Mw = 7.5

Source	Corner location of the fault		Length(km)	Depth (km)	Width(km)	Strike (^{o})	Dip	Rake(o)	Slip (cm)
	Longitude	Latitude							
1.00	120.00	20.00	277.00	40.00	34.67	20.00	41.00	79.00	50.12
2.00	119.51	17.20	254.00	40.00	34.67	1.00	36.00	95.00	
3.00	119.46	15.00	238.00	40.00	34.67	359.00	40.00	98.00	
4.00	120.65	12.85	190.00	40.00	34.67	310.00	25.00	90.00	

Mw = 7.0

Table 3: Geological parameters for each seaquake intensity

These parameters are vital for input parameters in TUNA-M2 to simulate the tsunami wave profile based on each of every seaquake intensity by moment magnitude. The maximum achievable wave height and period is recorded to further use it inside the SACS 5.3 software to simulate tsunami wave loading as solitary wave.

3.2. Attenuated lateral ground acceleration calculation.

Since the distance of the epicenter and the structure is far, the ground acceleration will be further reduced as the seismic waves travel through the earth's crust and thus lose energy. This ground acceleration can be further estimated by using a formula suggested by (AULOV & LIEW) where an empirical formula was developed to predict the attenuating ground acceleration that can only be used for all SHA in Malaysia. The formula that is going to be used are as follows.

For Shallow subduction zone (occur at the interface or contacting sides of two plates. Usually depth less than 70km).

$$l_n\,(PGA) = C_1 + C_2M_w + C_3M_w^2 + C_4D_e + C_5D_e^3 + C_6\,l_n\,(De + e^{C7Mb}) + C_8h + C_9H_3$$

of where

PGA	**Peak Ground Acceleration, in g**
M_w	Intensity of Earthquake by Moment Magnitude
M_b	Body-Wave Magnitude
D_e	Epicentral Distance, km
H	Depth, km
C1 – C9	Constants

The following table below are the related constant that is needed to be inputted into the equations.

C1	C2	C3	C4	C5	C6	C7	C8	C9
-28.778	3.18	-0.147	-0.002	0.000000000008314	0.295	1.026	0.198	-0.00004771

Table 4: Constant from C1-C9

3.3 Input for seismic analysis in SACS

There are four important parameters that need to be considered which are the ground acceleration (which is calculated by using formula in 3.2), overall modal damping, the soil type, and the fluid damping.

Overall modal damping is taken by 3% or 0.03 and fluid damping is ignored in this study. A poor soil will experience soil liquefaction of where a saturated, unconsolidated soil turns to a suspension of water when during an earthquake. Thus, the soil will lose some strength and behave more like a “liquid” and not retaining the structure anymore. It is important to make sure that the soil type is taken into account in this study. The soil parameters are given by PETRONAS inside psiinp.file and shall be readable by SACS.

3.4 Analyzing Respective Effects of the loading.

By using static analysis with non-linear pile/structure interaction, the ground acceleration of each of the seaquake’s magnitude is carried out concurrently with the tsunami wave loading upon the structure. At any point where the DAF (dynamic amplification factor) exceed by 110%, dynamic analysis should be taken into consideration and not by static analysis.

For this analysis, SACS software will analyze all eight direction; each of every 45^{o} and three loading types simultaneously on the structure as shown in figure 10. From here Postvue will produce the relative displacement on the members, moment and forces. Thus, the author can retrieve the maximal mean leg displacement and maximal total forces that can be further justified in this study.

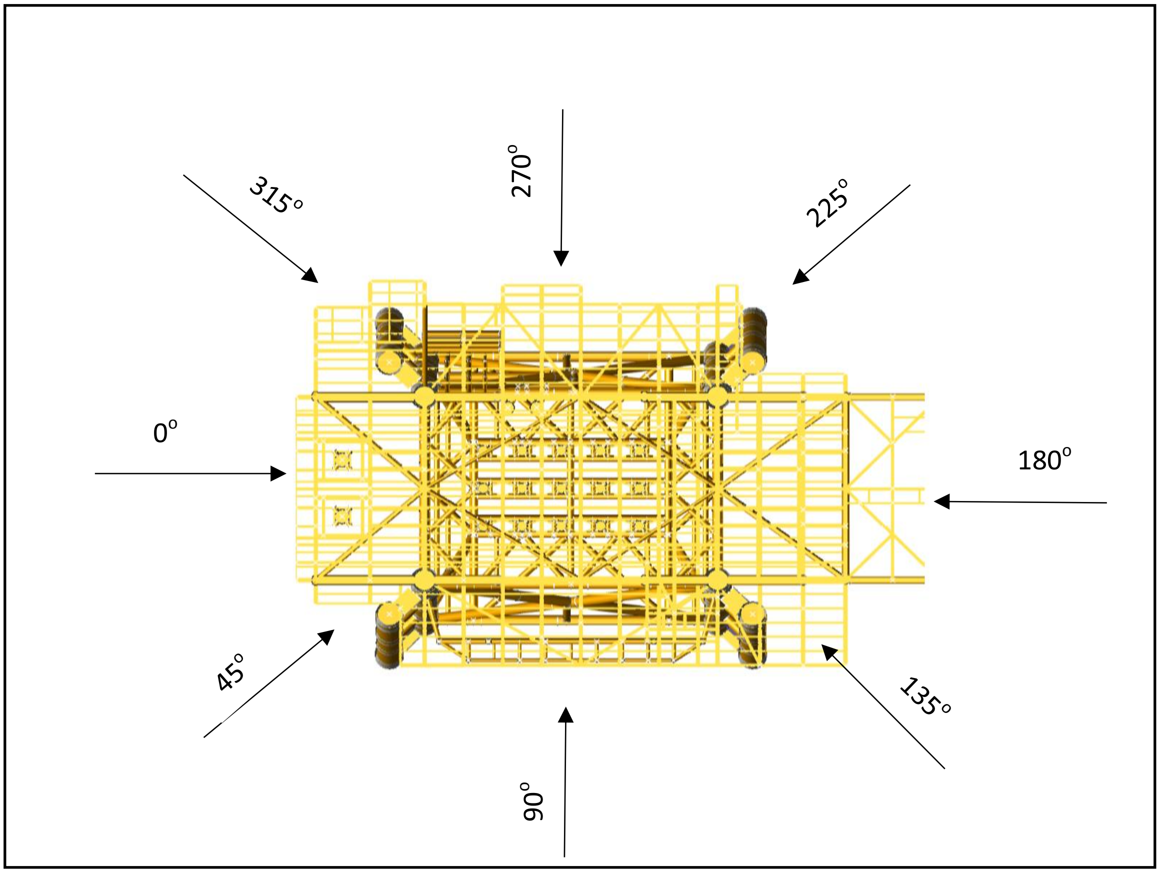

Figure 10: Loading direction for BADP-G

3.5 Determining the structural integrity.

The structural integrity of the platform shall be assessed on every seaquake intensity by using static linear analysis. If none of the members exceed the yielding stress capacity, the seaquake intensity is further increase by 0.5+ and the process continues. Should any of the members start to yield and the dynamic amplification factor exceeds more than 110%, a pushover analysis will be done to the platform.

From here, the base shear of the structure will be checked against the design base shear of the structure by RSR. The RSR value should not be less than 1.32 as per PETRONAS Carigali's recommendations. The overall flow of the methodology is shown in figure 11 below.

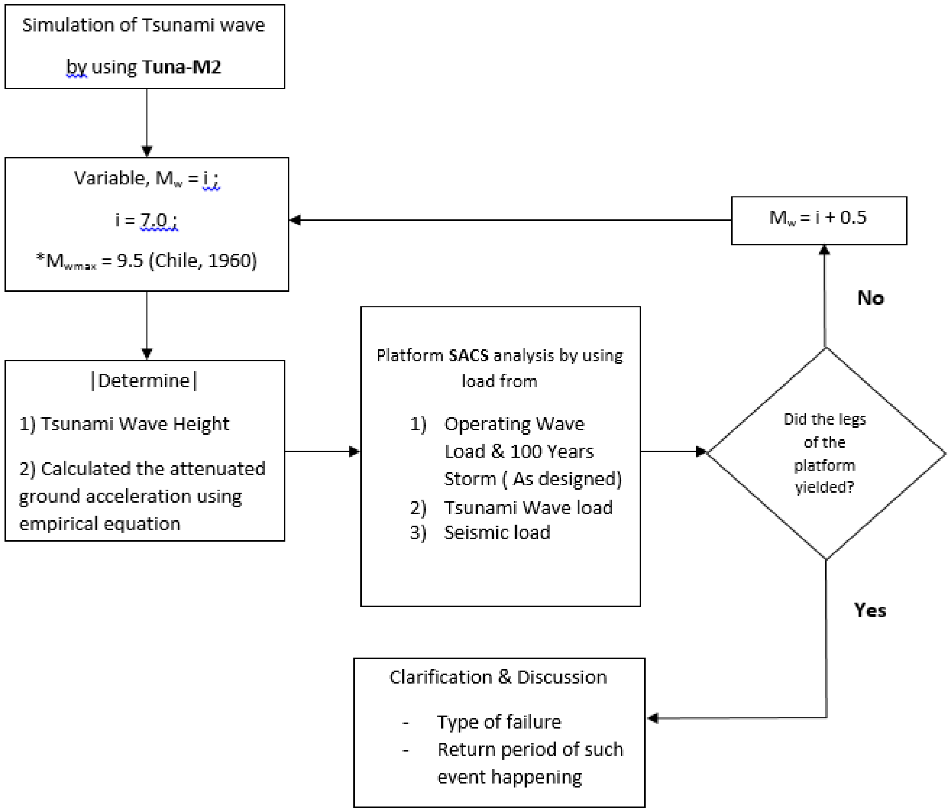

s

Figure 11: Flow chart of the study activity.

3.6 Project Activities

The study's detailing of major activities is represented by using a Gantt chart throughout the progress of the Final Year Project 1 in the figure 12 below. The Key Milestone had been already highlighted carefully based on figure 9 in the previous part of the report.

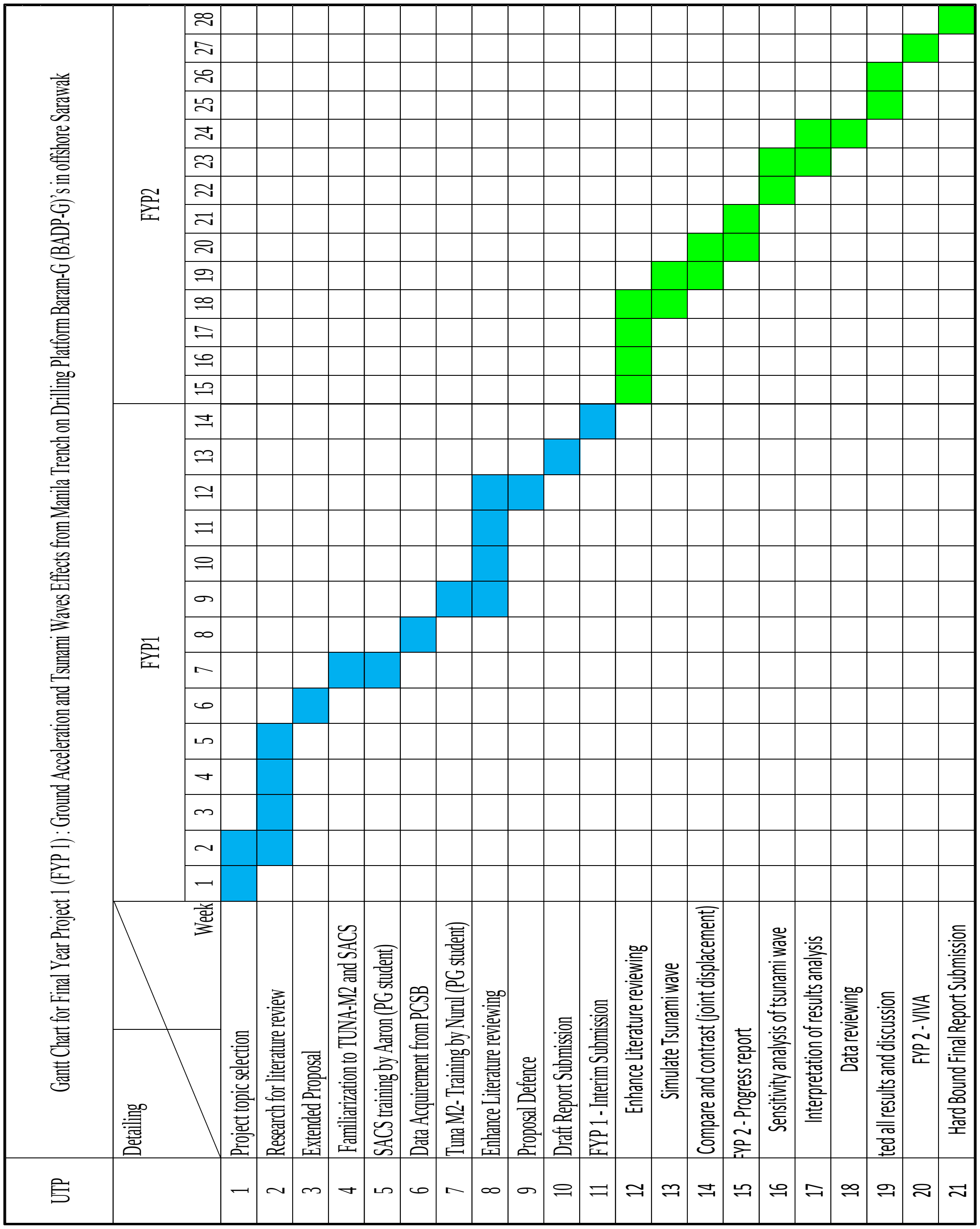

Figure 12: Project Gantt Chart.

4. Results and Discussion

4.1 Tsunami simulation results

The results of the tsunami wave generated by Tuna-M2 will be based on several geological parameters that has been mentioned in the report previously. The parameters such as coseismic slip of the fault, the depth, the width and etc pretty much govern of how much the resultant simulated tsunami wave height. To measure an accurate result of the tsunami wave height, the software allows to place control points (CP) which are points that is used to measure the wave height of the wave on a particular coordinates on a map which what is known as bathymethy. In achieving an accurate result of the tsunami wave height, four control points are placed surrounding BADP-G platform enclosing it in the middle, and thus an average results of the wave height is recorded on each of the control points.

The simulation of the wave height in the particular study is using an iteration of 1 until 40001 of taking the wave height on each moment of the time which last about 11 hours. During this time, a number of wave height is plotted into a spreadsheet then it is represented in a graph form on depending upon six moment magnitude (7Mw, 7.5Mw... until 9.5Mw). Early hypothesis is the higher the moment magnitude will yield a higher wave height of the tsunami. Figure below are the results of the simulated tsunami wave heights depending upon the magnitude of the earthquake by moment magnitude (Mw) and a table of the average maximum height of the tsunami waves for each magnitudes.

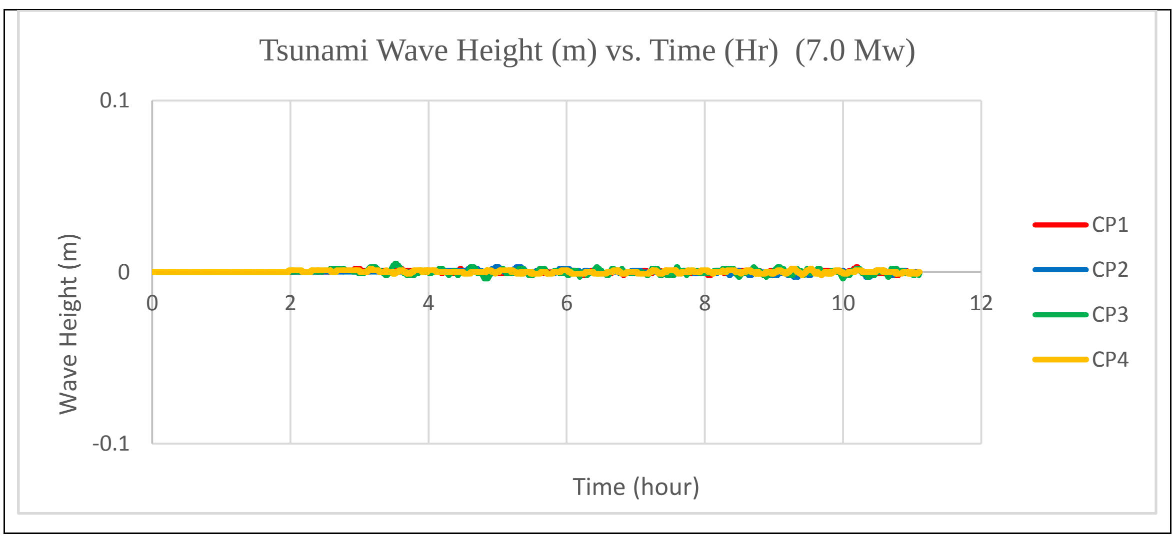

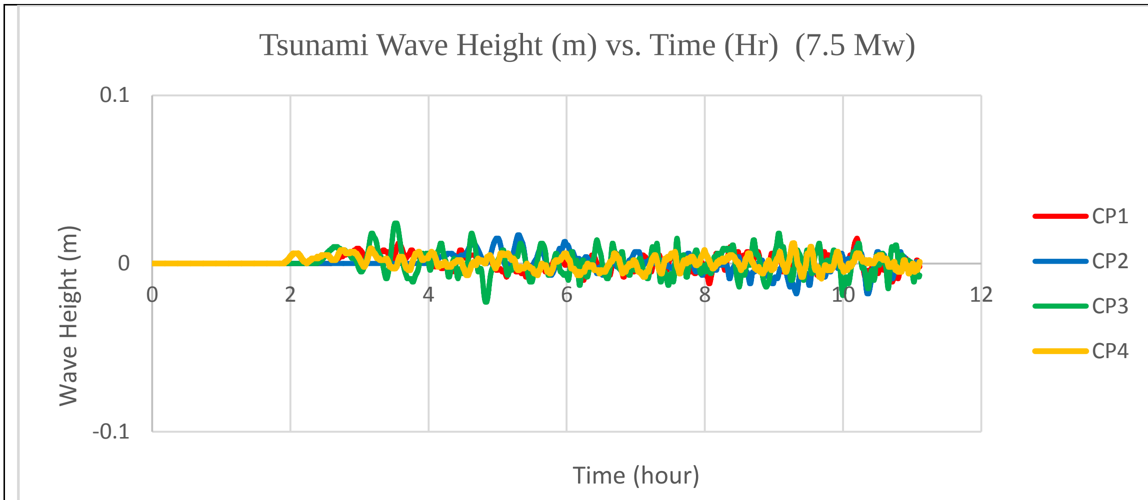
Tsunami Wave Height (m) vs. Time (Hr) (7.5 Mw)
0.1
0
-0.1
0
2
4
6
8
10
12
Wave Height (m)
Time (hour)
CP1
CP2
CP3
CP4

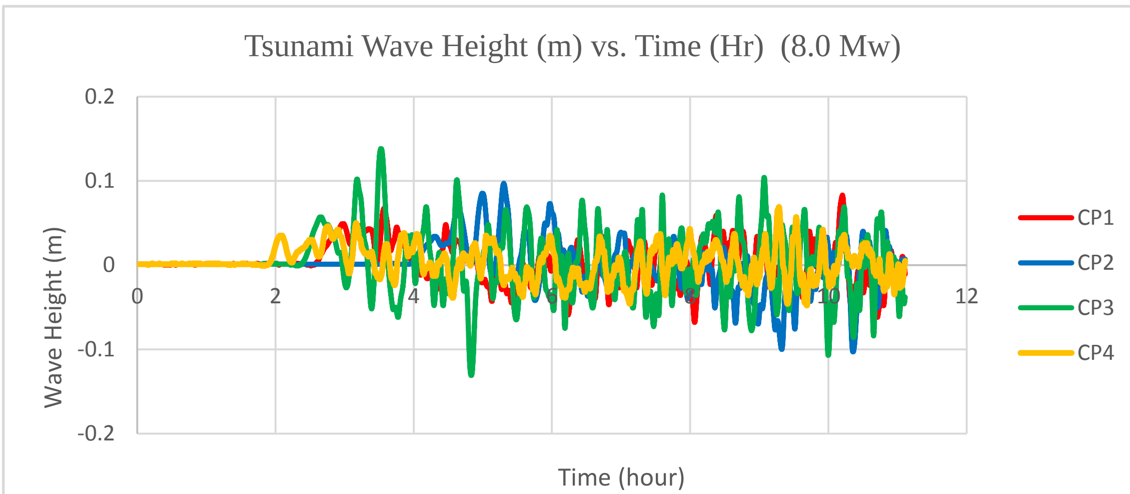
Tsunami Wave Height (m) vs. Time (Hr) (8.0 Mw)
0.2
0.1
0
-0.1
-0.2
0
2
4
6
8
10
12
Wave Height (m)
Time (hour)
CP1
CP2
CP3
CP4

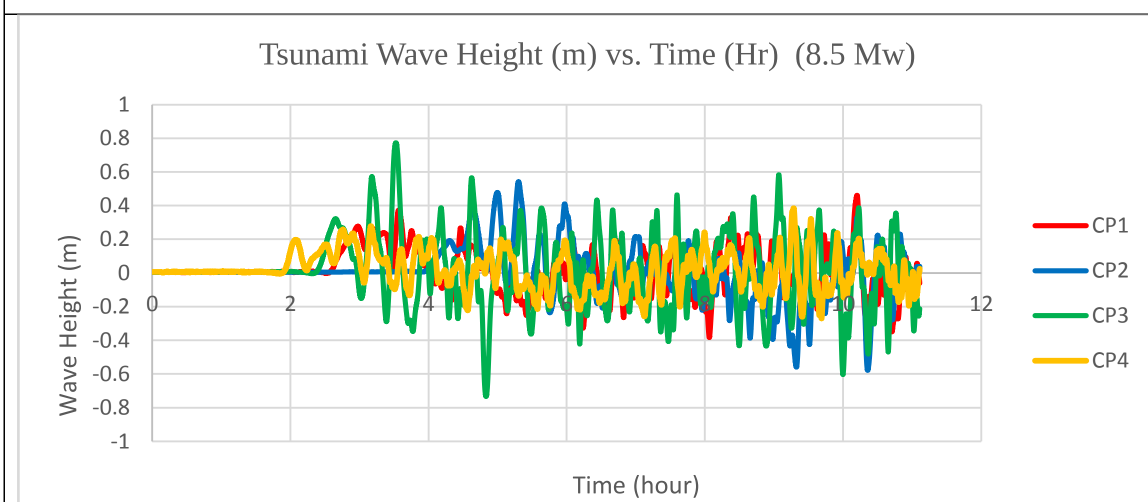
Tsunami Wave Height (m) vs. Time (Hr) (8.5 Mw)
1
0.8
0.6
0.4
0.2
0
-0.2
-0.4
-0.6
-0.8
-1
0
2
4
6
8
10
12
Wave Height (m)
Time (hour)
CP1
CP2
CP3
CP4

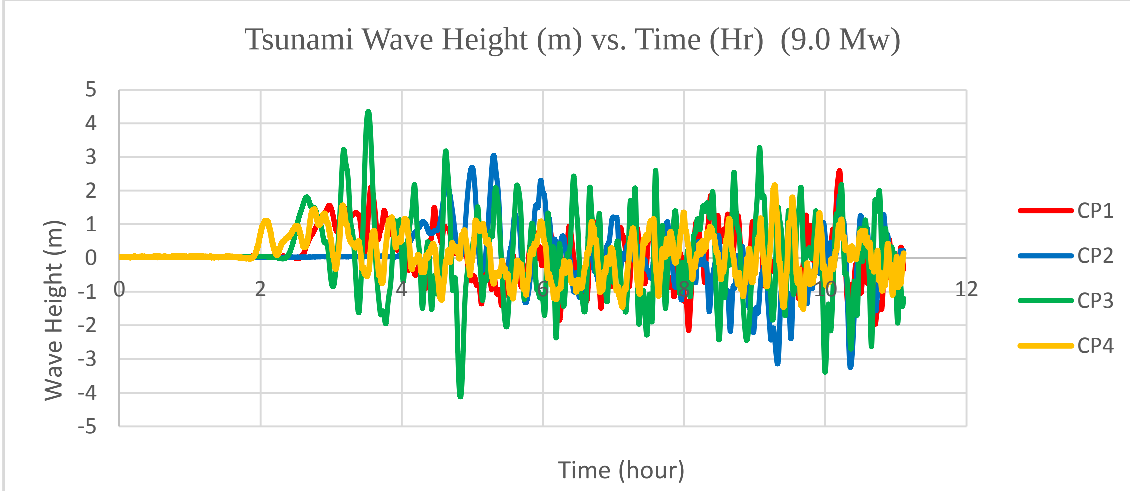

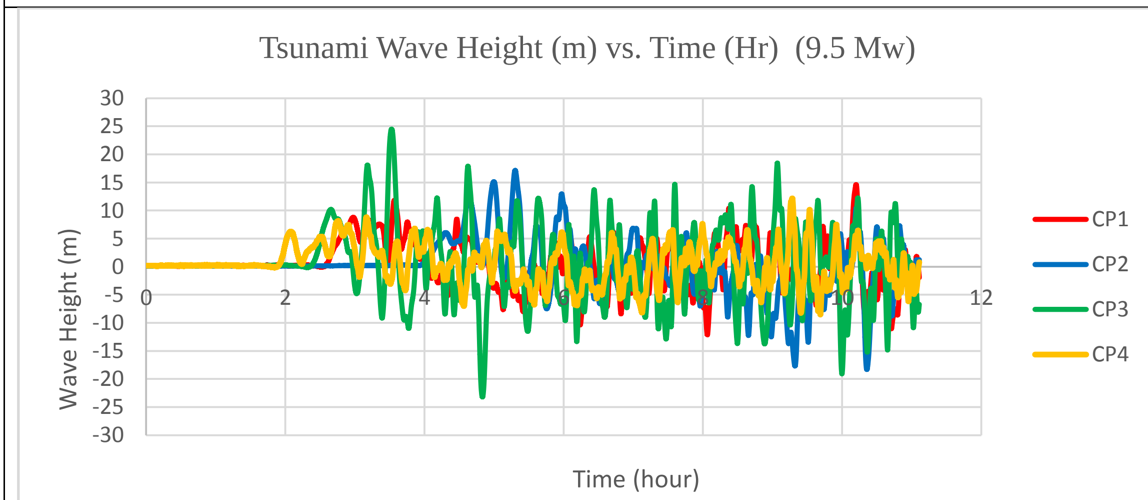

Moment Magnitude (Mw)	CP1 Max Tsunami Wave Height (m)	CP2 Max Tsunami Wave Height (m)	CP3 Max Tsunami Wave Height (m)	CP4 Max Tsunami Wave Height (m)	Average Max Tsunami Wave Height (m)
7.0	0.0030	0.00300	0.00500	0.00200	0.00330
7.5	0.0150	0.0170	0.0240	0.0120	0.0170
8.0	0.0830	0.0970	0.138	0.0690	0.0980
8.5	0.461	0.542	0.773	0.384	0.540
9.0	3.194	3.375	4.815	2.404	3.447
9.5	14.589	17.133	24.457	12.154	17.080

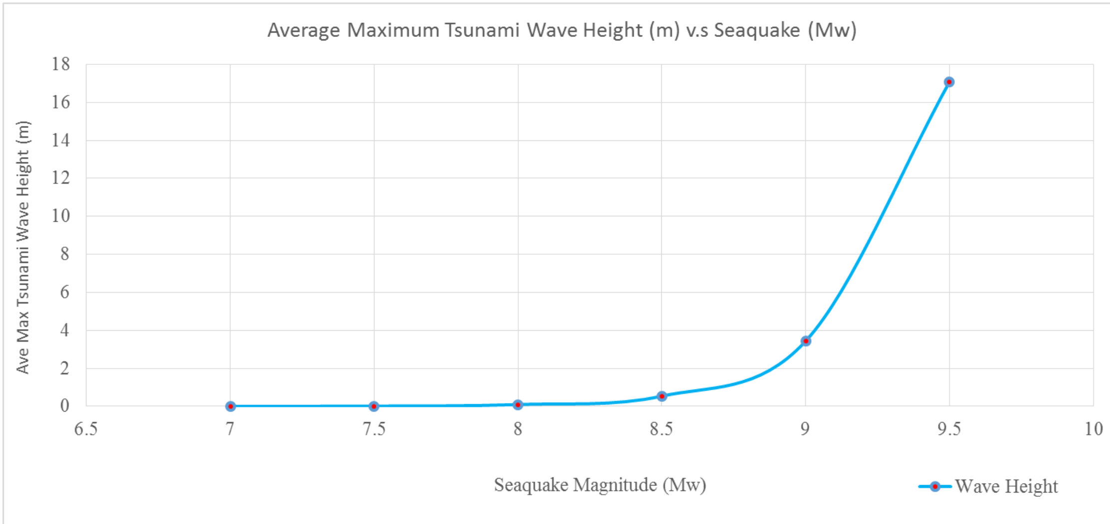

Figure 13 and Table 5 : Tsunami wave height (m) versus time (hr) and results of average maximum tsunami wave height (m)

As what has been stated before, the average maximum tsunami wave height is taken to average from four different control points that is surroundings of the platform to accurately predict the tsunami wave height.

However, not all of the seaquake magnitude seems to be a hazard to the platform. For example, magnitude of 7.0Mw yields an average maximum tsunami wave height of 0.003m which is negligible. This also applies to 7.5, 8.0 and 8.5 which resulted to a very small tsunami wave height if to be compared with operating condition of the platform (in the next sub-topic). When the seaquake magnitude hits 9.0 by moment magnitude, it yield an average maximum tsunami wave height of 3.45 meters which is higher than the significant operating wave height.

Then again, the highest possible seaquake magnitude will be at 9.5Mw which yield the highest wave of 17.08meters. This is most critical wave height as the wave height is about 1.7 times higher than 100-year storm event for the maximum wave height and thus making the structure prone to failure.

It is seemly justified that the magnitude of the seaquake does affect the tsunami wave height. As the seaquake magnitude increases by moment magnitude, the tsunami wave height increases exponentially. But after the seaquake hit 9 Mw magnitude, the graph starts to increase directly proportional to the average maximum tsunami wave height (m). Thus, it is reliable enough to produce another separate graph by linear interpolation which covers seaquake magnitude from 9Mw until 9.5Mw. It is strictly suggested that the equation of the graph below is only valid throughout seaquake magnitude ranging from 9-9.5Mw and not from 7Mw to 9Mw since the equation of the tsunami wave height from the range aforementioned is rather exponential initially. The graph then can be used to determine the sensitivity of the tsunami wave height against the seaquake magnitude by using a straight graph especially seaquake magnitude ranging from 9Mw onwards.

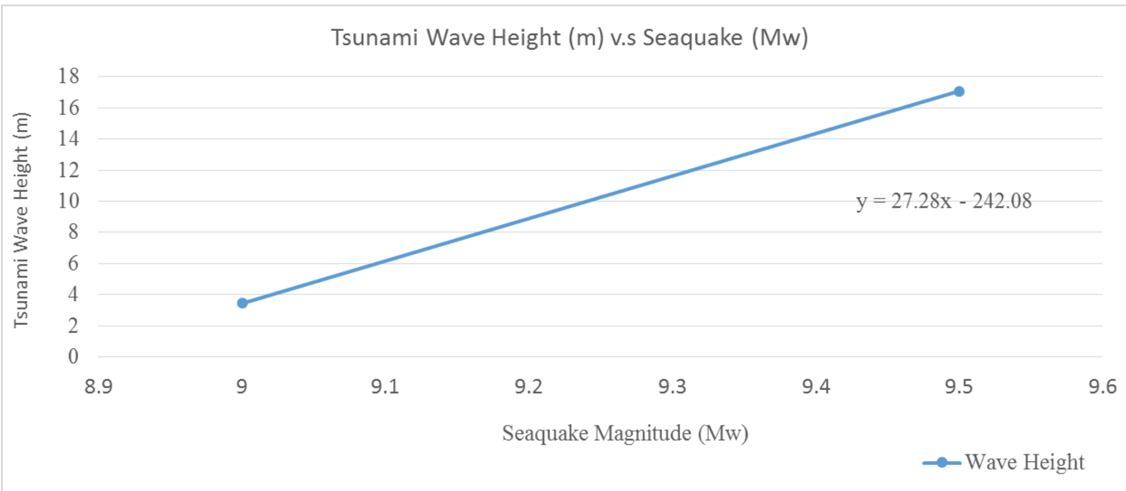

Figure 14 : Tsunami wave height against seaquake of 9.0Mw onwards.

Due to the limitation of the TUNA-M2 software, the wave period cannot be obtained directly from the software and be plugged into SACS 5.3. However, the analysis is using the wavelength of 10000 meters to satisfy the wavelength of tsunami since it is very big, and thus can be accounted as infinite (Pararadarayannis, 2001).

4.2 PETRONAS Technical Standards (PTS) and local study parameters.

The design of fixed offshore platform in Malaysia is mainly governed by the extreme storm of a 100-years storm event. Thus, PETRONAS has set a recommended parameters for environmental loading to be applied for the design of the platform. In PTS, under clause L.1.3 Wave parameters of Baram Delta field, it states generally the highest wave height for the operating criteria and 100-year storm event for any platform with water depth of 75m at Baram field. The parameters is shown in the table below.

Parameters	Operating Criteria	100-year storm event
H_{max} (m)	6.5	10.0

Table 6 : Clause L.1.3 of PTS. Wave parameters of Baram Delta field.

But this platform is eventually have its own operating criteria and 100-year storm highest wave height value since the water depth is 15.5m which is nowhere near to the PTS water depth for Baram field (75m). Thus, based on local study of a defaulted value of Hmax provided inside the sacinp file, the value for each of the Hmax is provided in the table below, different for every direction.

Hmax (m) based on direction of wave	Operating Criteria (m)	100-year storm event as per designed (m)
0	4.2	6.6
45	1.6	2.4
90	1.6	2.4
135	3.4	4.6
180	4.2	6.6
225	5.6	7.6
270	5.6	7.6
315	5.6	7.6

Table 7 : The maximum wave height for operating and 100-year storm based on the directionality of the wave.

As what can be seen from the table above, the operating criteria and 100 years storm is not constant and will be depending upon the direction of wave. The decision to these numbers are based on local study that was established for this special platform at Baram field and what makes it special because of a smaller water depth compared to the other platform around Baram field. Therefore, it is not possible to simply decide on the most severe direction of the tsunami wave based on the value above. Thus, lateral forces on the platform will further be checked so that determination of most severe direction of wave can be determine for sensitivity checking towards incrementing tsunami wave height

4.3 Lateral forces due to operating wave and 100 years storm wave.

Before any loading is applied to the platform, four members at the leg primarily are chosen to determine its reaction toward the related forces. The reason being the main legs are selected is because these four legs are the main support which will be supporting the topside, drilling equipment, any workers and etc. The figure shown below are the positions of the selected members on the platform that will be analyzed. Another table is shown to present briefly the members join

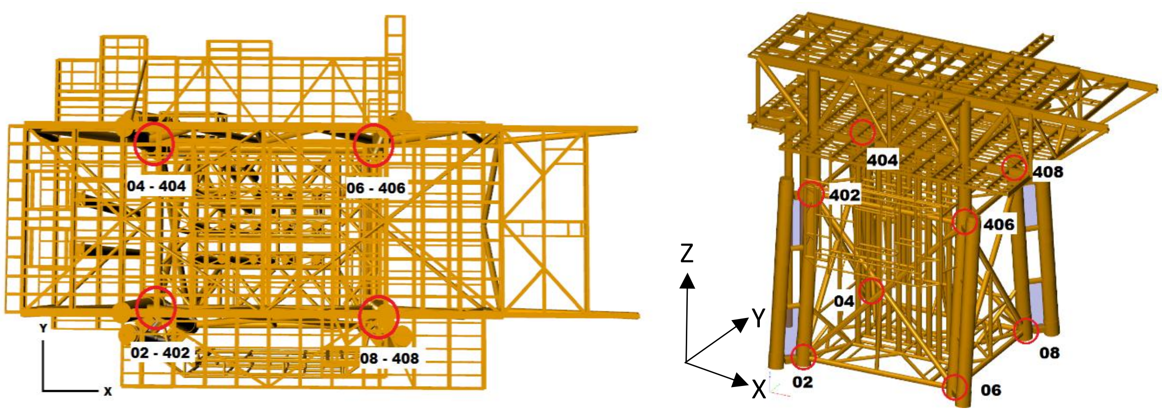

Member	Joint A	Joint B	Length (m)
Leg 1	02	402	18.737
Leg 2	04	404	18.737
Leg 3	06	406	18.737
Leg 4	08	408	17.737

Figure 15 and Table 8 : BADP-G top view & isometric view and summary of selected leg members.

The analyzation of the platform is calculated by using SACS 5.3. The load condition is selected under certain name like OP01 (Operating Load condition 1 @ 0 Degree) and ST01 (100 years storm condition 1 @ 0 Degree) of where all the wave characteristics such as period, wave height, wave type, kinematic factor, wavelength and etc are defined inside the software. All of the wave and plus the current forces for both operating and 100 year wave storm are under seastate environmental loading where it is statically loaded to the platform.

Directions	Operating Wave ∑F (KN)	Storm 100yrs ∑F (KN)	Difference in ∑F (KN)
0º	3135.00	5930.40	2795.40
45º	1100.46	1986.03	885.57
90º	662.05	1436.86	774.81
135º	1635.61	3068.97	1433.36
180º	2029.17	4150.60	2121.43
225º	3045.56	6065.12	3019.55
270º	3131.41	5940.16	2808.75
315º	4614.81	8037.06	3422.25

Table 9: Summation of forces for operating and 100 years storm

The table above shown above is to present the normal operating wave load and the 100 years wave storm from every directions surrounding the platform. The summation of forces is calculated by using Pythagoras theorem of two dimensional forces of Fx and Fy since Fz does not contribute to the lateral forces to the platform. From the table above it is clear that the highest force is coming from 315º degree of which 4614.8 KN and 8037.06 KN for operating and 100 years storm wave force.

4.4 Maximum Displacement of joints due to operating and 100 years storm wave forces.

The maximum displacement of joints is presented as per table below.

load	Joint Name	Total Displacement (cm)	load	Joint Name	Total Displacement (cm)
0 (OP)	312X	25.11	0 (ST)	312X	41.90
45 (OP)	312W	5.12	45 (ST)	312W	6.91
90 (OP)	726	1.24	90 (ST)	726	2.95

135 (OP)	312X	7.34	135 (ST)	312X	9.48
180 (OP)	312X	14.03	180 (ST)	312X	23.26
225 (OP)	312X	20.18	225 (ST)	312W	35.90
270 (OP)	312W	21.47	270 (ST)	312W	27.35
315 (OP)	312X	28.16	315 (ST)	312X	35.93

Table 10: Maximum joint displacement for operating and 100 years storm force.

When the operating wave loading and 100 year storm wave forces are exerted to the structure, three joints were identified to yield the highest joint displacement inside the system. The joints are 312X, 312W and 726. The problem is that these joints are members which does not contribute to the integrity of the structure. SACS 5.3 is capable to highlight these type of member in blue to indicate these “dummy structures” such as gas risers. Risers for example is a conduit to transfer any substance from the seabed up to the water surface. It is simply similar to flow lines of where riser will be used to transfer oil, gases, control fluid and injection fluid and obviously it does not help to transfer any loading to the structure but rather use for hydrocarbon transportation. Thus, in correlating with the three joints above, 312X and 312W are riser’s joint meanwhile joint 726 is a joint at the topside which can also be considered as dummy structures.

4.5 Determining the most severe directional wave based on joint displacement of the legs.

Since the maximum joint cannot be accounted for the wave loading, it is essential to only focus on the joint at the four legs. The total displacement of joints is calculated by subtracting the displacement after the platform is loaded with 100 years storm wave with the displacement after the platform is loaded with operating wave loading. From here, the total displacement can be seen based on how much the joint has been displaced after the normal condition platform changed to the extreme condition of the wave.

The idea of acquiring the worst direction of wave to the platform is by simply selecting the direction which has the highest joint displacement value provided if the 100 year wave storm is omnidirectional; same wave height in every directions. In this case, the 100 year wave storm is not the same for every direction of the wave. For example, based on the local study for 100 years wave storm with a directionality of 180 degree is having a 6.6meter wave height compared to 270 degree which has 7.6m of wave height. The problem is quite clear here. Let just say that assuming joint X at the leg of the platform will be loaded with storm wave loading at a direction of 180 and 270 degree at a 6.6m and 7.6m wave height respectively. After the platform is loaded, the displacements for joint X is 1.79cm and 1.74cm respectively. Logically thinking, a higher wave height will results to a higher force and yield the highest displacement but this is not truly the case. In structural point of view, the redundancy, configuration and properties of the members locally will govern on how much the joint will deflect.

Apparently, the structure cannot be loaded with different wave height in determining the worst direction of the platform. Thus, the platform will be loaded with the highest value of 100 years storm wave of 7.6m in wave height for all directions (omnidirectional). Moreover, the joint displacement value is rather consistent since the wave height is kept constant for all directions and the highest joint displacement value will be selected as the most severe direction.

Joint displacement @ legs (cm) , by 7.6m 100 years wave storm								
Directions	Leg 1		Leg 2		Leg 3		Leg 4	
	2	402	4	404	6	406	8	408
0º	4.54	4.51	4.57	4.52	5.86	5.86	5.81	5.76
45º	3.08	3.01	3.15	3.13	4.10	4.06	4.17	4.04
90º	1.34	1.31	1.36	1.37	1.78	1.73	1.83	1.73
135º	1.31	1.34	1.28	1.31	1.60	1.56	1.62	1.61
180º	1.26	1.38	1.17	1.30	1.48	1.61	1.45	1.59
225º	2.94	3.08	2.56	2.74	3.34	3.54	2.99	3.19
270º	4.11	4.11	3.88	3.83	4.58	4.61	4.27	4.31
315º	**5.30**	**5.33**	**5.31**	**5.24**	**6.47**	**6.47**	**6.34**	**6.37**

Table 11: Joint displacement at four legs under 7.6m 100 years wave storm

In the table above, it is clearly to say that the worst direction for this platform is 315 degrees since it yield the highest joint displacement for each of every legs.

4.6 BADP-G sensitivity analysis on tsunami wave loads

In the previous topic, it is safe to say that the most severe direction for the BADP-G platform is approaching from 315 degree. Thus, the analysis will be done solely based on only for this directions since presuming that the direction aforementioned is the most prone towards incoming tsunami wave loading.

In subtopic 4.1, tsunami wave height was acquired through simulation based on several geological parameters by using TUNA-M2 software. The tsunami wave height is tabulated below based on each and every seaquake magnitude starting from 7Mw until 9.5Mw.

Seaquake magnitude (Mw)	Tsunami Wave Height (m)
7	0.00033
7.5	0.0017
8	0.098
8.5	0.54
9	3.45
9.5	17.08

Table 12: Tsunami wave height depending upon the seaquake magnitude

Based on the previous discussion, the design of the platform is governed by the 100 years wave storm which is 7.6m in wave height for 315 degree in direction. On the table 12 above, a tsunami wave height from 7Mw until 9Mw can be theoretically negligible since the tsunami wave height is out of the range of the design 100 years storm wave which is 7.6m. Apparently, it falls in the region from 9Mw until 9.5Mw and thus, the sensitivity analysis shall start from 7m tsunami wave height up to where four of the platform legs fails.

Member failure shall be determine through the member's maximum unity check of which any member's UC exceed 1 is considered as fail due to the member plastic behavior.

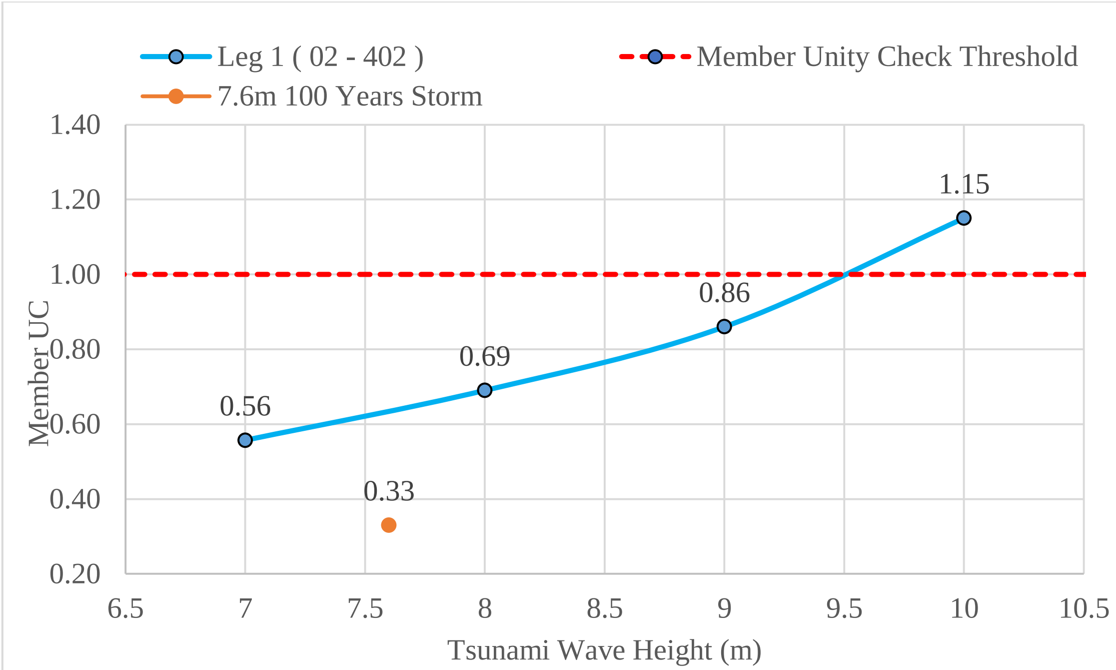
Leg 1 (02 - 402)
Member Unity Check Threshold
7.6m 100 Years Storm
Member UC
1.40
1.20
1.00
0.80
0.60
0.40
0.20
1.15
0.86
0.69
0.56
0.33
6.5
7
7.5
8
8.5
9
9.5
10
10.5
Tsunami Wave Height (m)

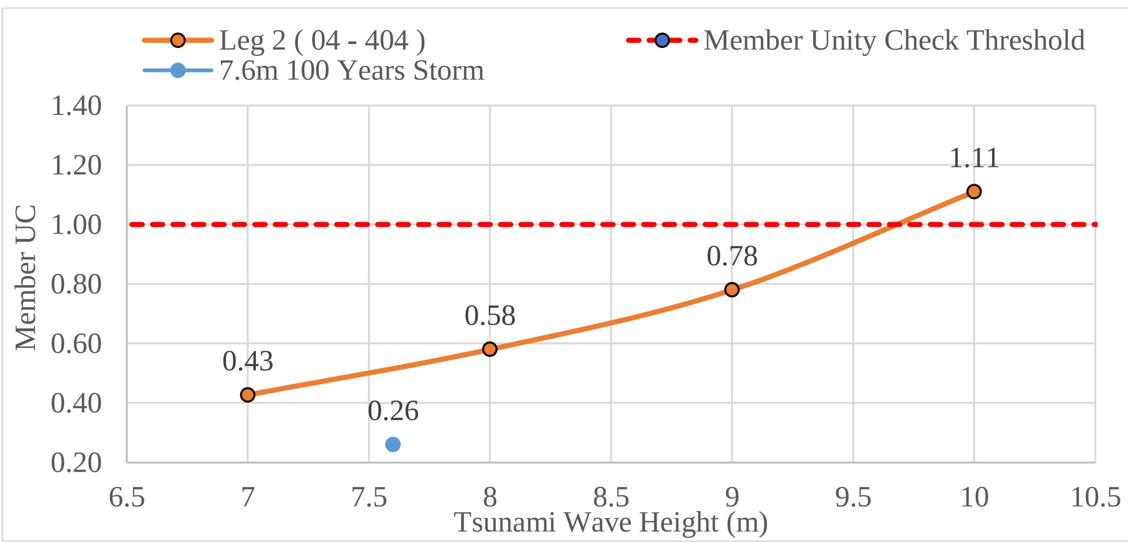
Leg 2 (04 - 404)
Member Unity Check Threshold
7.6m 100 Years Storm
Member UC
1.40
1.20
1.00
0.80
0.60
0.40
0.20
1.11
0.78
0.58
0.43
0.26
6.5
7
7.5
8
8.5
9
9.5
10
10.5
Tsunami Wave Height (m)

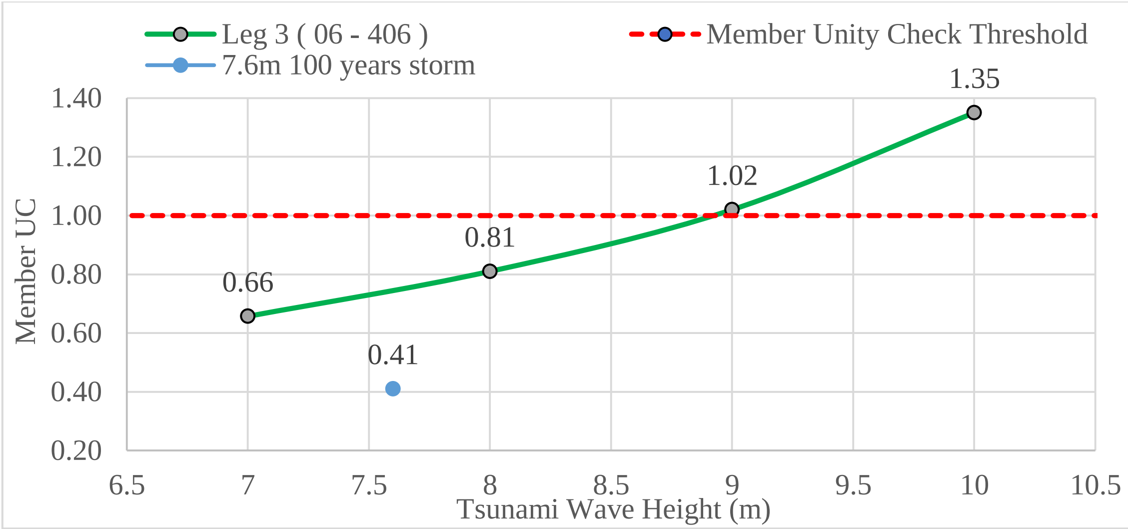

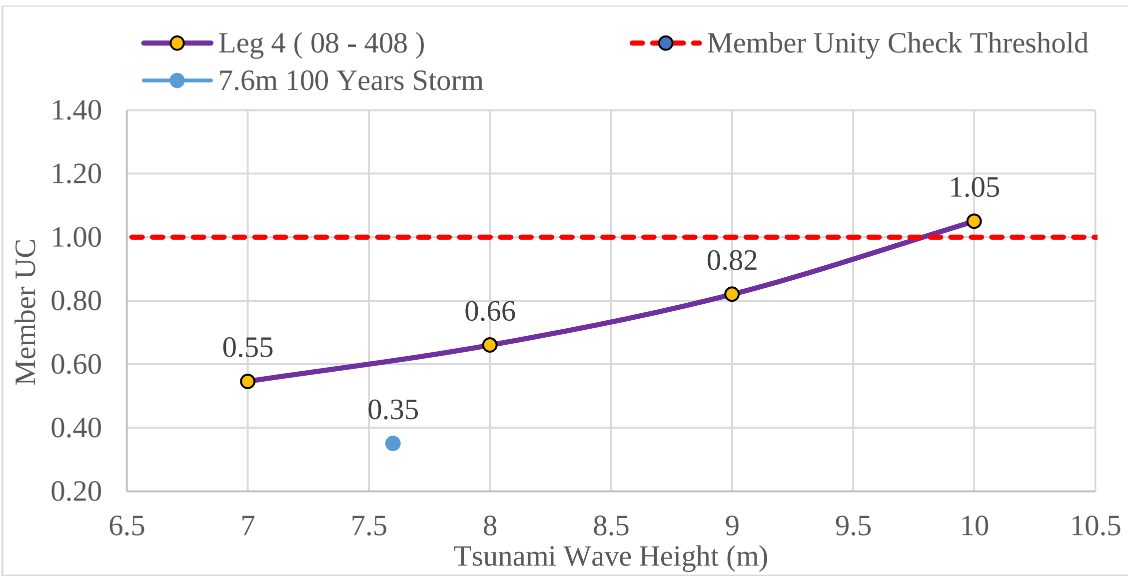

Figure 16: Member unity check for four platform legs

Figure 16 shows four graphs representing the unity check for each leg members. There are 2 main elements inside the graph which need to be highlighted such as the increment of each of the member's unity check as the tsunami wave height increases from 7m until 10m and another member's unity check at where the 100 years wave storm is. Eventhough the wave height for the 100 years storm is 7.6m which is much higher than the first 7m tsunami wave height, it can be seen that all of the unity check for the tsunami wave height is higher compared to the 100 years storm. This is because tsunami wave height is a shallow type of water wave and the wave loading act differently compared to the 100 years storm wave. Even tsunami wave loading calculation was based on solitary wave theory and not stokes as what has been practice for normal water waves.

Since the analyzation does not include collapse analysis, technically the structure's survivability should jeopardized when all the platform legs unity check exceed 1. To deduce the phenomenon above, at a threshold of 9m tsunami wave height, it can be seen that leg 3 reached its plastic limit state of where its unity check had exceeded 1 (UC leg 3 = 1.02). The member failed in compression due to the crushing force of the platform towards leg number 3. However, leg 1,2 and 4 is still resisting almost 80% of their ultimate load capacity at 9m tsunami wave height.

When the tsunami wave height had reached 10 meter, all of the four legs member unity check exceeds 1 of where the highest was 1.35 for leg number 3. In this state, the platform legs are plastic in nature and shall not able to carry any loading. Since the tsunami wave load is approaching 315 degree, the wave load pushes leg number 2 away making it failure in tension and bending meanwhile member failure by compression can be seen for leg number 1, 3 and 4. The table shown below is the summation of forces of the tsunami and 100 years storm wave at 7.6m

Tsunami Wave Height (m)	Fx (KN)	Fy (KN)	∑F (KN)
100 YRS STORM (7.6)	5519.84	-5841.72	8037.06
7	7120.66	-7377.97	10253.69
8	8903.43	-9248.01	12837.32
9	11130.29	-11589.3	16068.47
10	14450.94	-15071.7	20880.26

Table 13: Summation of forces of the tsunami and 100 years storm wave load

At a 10 meter tsunami wave height, the wave force exerted to the platform at 315 degree direction is 20880.26 KN. In other word, the platform will fail when the incoming tsunami wave force is 2.6 times higher than the designed 100 years storm wave load.

4.7 Attenuated lateral seismic loading.

By using geological parameters that was used to simulate the tsunami wave height in chapter 4.1, the peak ground acceleration is hand calculated using an empirical formula developed by Aulov, A. (2013) based on the distance from epicenter to the platform (1220kilometers away). The PGA is represented into a graph and shown below.

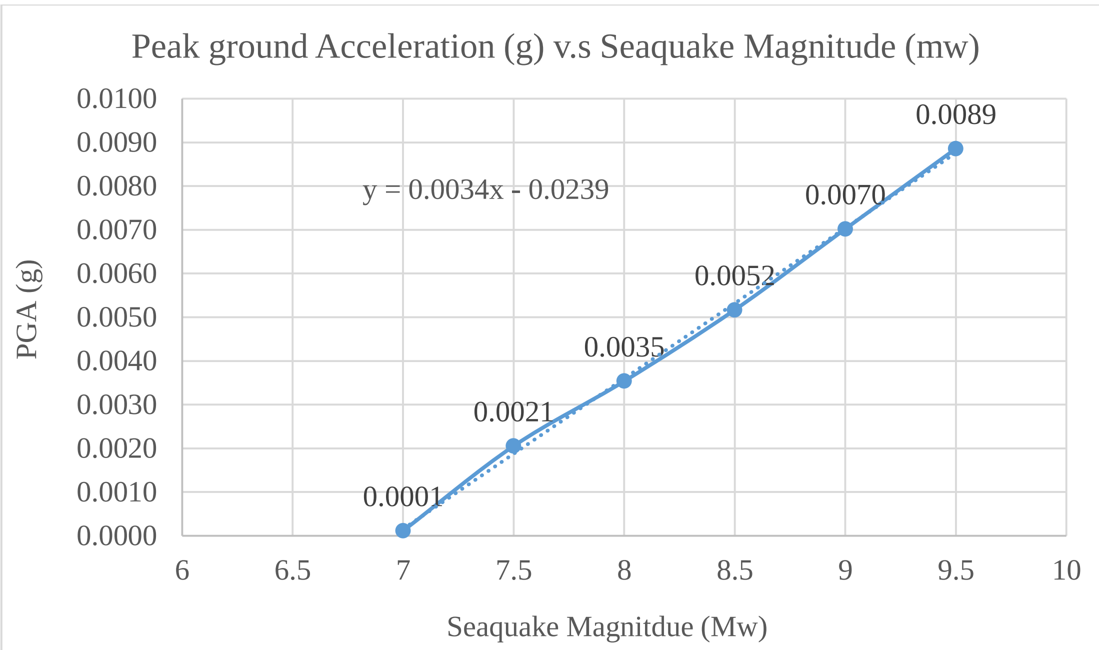

Figure 17: PGA (g) v.s Seaquake magnitude (Mw)

Apparently, the highest peak ground acceleration value was 0.0089g at 9.5Mw (highest achievable earthquake magnitude) of where the value itself is too small to be incorporated into the design. Following the API RP 2A WSD, clause 2.3.6b for zone of low seismic activity, any areas of where the peak ground acceleration value is less than 0.05g, no analysis is required (API, 2000). Thus, seismic lateral loading is not going to affect the integrity of the structure because it is negligible.

4.8 Return Period

In the paper of “Effect of tsunamis generated in the manila trench on the gulf of Thailand” ,of where in a general study of the events of earthquake for Manila Trench were collected from the Advanced National Seismic System is then analyze by using Gutenberg-Ritcher recurrence law to produce an annual rate of exceedence graph against the earthquake magnitude (Ruangrassamee & Saelem, 2009). The data of the magnitude against return period in years are shown in the table below.

Magnitude	Return Period (Years)
7.0	6
7.5	19
8.0	63
8.5	205
9.0	667

Table 14: Return period for each magnitude

The graph is then re-plotted in a spreadsheet to obtain the equation of the graph of a return period in years against the earthquake magnitude in moment magnitude. Once the equation of the graph is obtained, it is possible to determine the threshold tsunami wave height of 9m and 10m return period to see on the occurrence of the tsunami wave height and plus the earthquake magnitude at which will yield wave height of 9m and 10m.

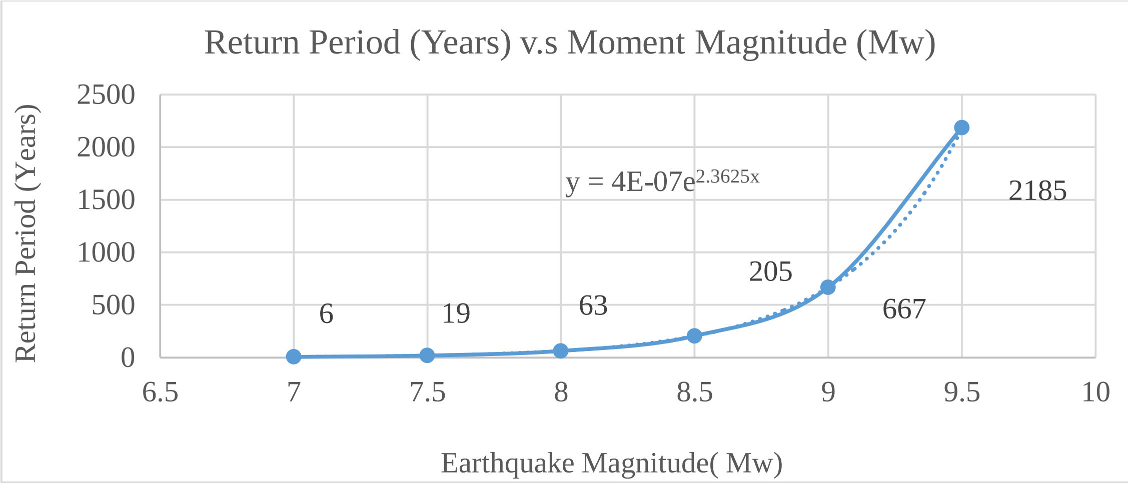

Figure 18: Return period (years) v.s earthquake magnitude (mw)

Reviewing back topic 4.1 which is tsunami wave simulation, by using an equation from a graph labeled in figure 14, the earthquake magnitude is calculated by using the equation $y = 27.28x - 242.08$ of where y is the tsunami wave height and x is the seaquake magnitude. Proceeding the determination of the return period of the tsunami wave height will be based on the equation in figure 18 which is $y = 4 \times 10^{-7e^{2.3625x}}$ of where y is the return period in years and x is the earthquake magnitude in moment magnitude based on the threshold of the tsunami wave height.

Tsunami Wave Height (m)	Seaquake Magnitude (Mw)	Return Period (Years)
7	9.13	932.5
8	9.17	1025
9	**9.20**	**1110.1**
10	**9.24**	**1211**

Table 15: The seaquake magnitude and return period for tsunami wave height (m)

Based on the value above it is worth mentioning that since the return period for 9m tsunami wave height is rather low (less than 1%), no mitigation action is needed for this platform but however early attention should be taken to ensure the operator shall be kept in vigilant on the potential tsunami wave loading.

Chapter 5

5.1 Concluding overview

This project addresses the issue of structural integrity doubtness of a Baram drilling platform-G by providing a sensitive insight into the phenomenon of tsunami wave loading and its attenuated ground acceleration with regards to the normal operating metocean criteria. The Manila Trench is one of the potential source of tsunami hazard in the Malaysian region which is still active and rupture is possible to produce tsunamis. The platform BADP-G was chosen to representative from Baram field to be tested against the tsunami wave loading and its seismic loading. In this case, the platform survivability is tested against checking the maximum leg member unity check, comparing as per designed with the tsunami wave load T joint displacement for all the legs, finding the failure mode for the legs and the annual rate of exceedence of such seaquake from happening.

The analysis used to analyze the platform is linear static with non-linear pile interaction as to follow the standard practice of oil companies do to assess offshore platform. However, pushover analysis is not applicable in the study because of a smaller scope of study. In the following, the project gives a general understanding on the structural response of the fixed offshore jacket when it is subjected to tsunami wave loading comparing to the normal operating and as per design criteria loading.

5.2 Results Executive Summary

1. The highest achievable tsunami wave height is 17.08meters high when the seaquake magnitude hits 9.5Mw and can be as low as 3.44meters of when the seaquake is 9.0Mw
2. Any seaquake magnitude lower than 9.0Mw will yield an insignificant tsunami wave height that can be ignored since the operating wave loading (6.6m) is much higher than any tsunami wave height obtained from 9.0Mw and below.
3. Seismic loading is negligible since the highest peak ground acceleration with the highest seaquake magnitude of 9.5Mw yield only 0.0089g of ground acceleration. API recommend that any seismic loading should have a value of at

least 0.05g of the peak ground acceleration to be considered into the design of the platform.

4. The most severe directional wave loading is 315 degree based on a 7.6m wave height of a 100 years wave storm since it yield the highest joint deflection for all eight joints at the legs comparable to the other 7 directions.
5. The threshold of the tsunami wave height is at 9m of where leg number 3 had reached its plastic limit (UC = 1.02) and the member failed in compression. For the other leg members are still resisting 80% of the total ultimate capacity loading for each of the member. The summation of forces exerted on the platform was 16068.47 KN.
6. At 10 meter tsunami wave height, all leg members gone through plastic limit state of which all of the member exceed unity check value of 1. Technically, the structure cannot withstand any loading from the tsunami wave load and all the legs will fail. The summation of forces exerted on the platform at this point was 20880.26 KN
7. The threshold tsunami wave loading of 9m will have a seaquake magnitude of 9.2Mw and a return period of 1110.1 years. The author suggested to the operator (PETRONAS) of no sudden mitigation action is required on this problem since the annual rate of exceedence is small (< 1 %) but rather be attentive and aware to the potential incoming tsunami wave that can destroy BADP-G platform in Sarawakian waters.

5.3 Recommendation

The case study conducted in the research can be further continued to include a full detailed dynamic analysis of a fixed offshore platform including non-linear pushover analysis. Since BADP-G platform is relatively placed on a smaller water depth, the chances are platform with a bigger water depth will behave differently compare to this platform. Thus, the author would strongly suggest to study for multiple platform surrounding Baram field with the differences in water depth in respect to the force of incoming tsunami wave loading.

In Malaysia, engineers are slowly incorporating seismic design into the design of a fixed offshore platform. Perhaps, the project can be further continued to be analyzed with a different source of seismic loading on a nearer geological fault such as Andaman trench, Sumatra in finding the structural performance against lateral ground movement on a different fault.

Lastly, another area that can be improved is to consider a different type of soil strength into the analysis so that a broader perspective in looking towards the effect of the strength of the soil on the structural performance under tsunami wave loading. Since damaged soil will have a weaker foundation for the structure compared to a good soil and will affect the integrity of the piling system in respect to sustaining tsunami wave force exerted to the platform.

References

API, R. (2000). *2A–WSD Recommended practice for planning, designing and constructing fixed offshore platforms–Working stress design.* Paper presented at the Twenty.

AULOV, A., & LIEW, M. S. Seismic Hazard Analysis (SHA) Considerations for South China Sea Territories of Malaysia.

Chakrabarti, S. (2005). *Handbook of Offshore Engineering (2-volume set)*: Elsevier.

CRUZ SALCEDO, J. (2011). EARTHQUAKE SOURCE PARAMETERS FOR SUBDUCTION ZONE EVENTS CAUSING TSUNAMIS IN AND AROUND THE PHILIPPINES. *Bulletin of the International Institute of Seismology and Earthquake Engineering, 45*, 49-54.

Dao, M. H., Tkalich, P., Chan, E. S., & Megawati, K. (2009). Tsunami propagation scenarios in the South China Sea. *Journal of Asian Earth Sciences, 36*(1), 67-73. doi: http://dx.doi.org/10.1016/j.jseaes.2008.09.009

Elnashai, A. S., & Di Sarno, L. (2008). *Fundamentals of earthquake engineering*: Wiley Chichester.

Ersdal, G. (2005). Assessment of existing offshore structures for life extension. *Department of Mechanical and Structural Engineering and Material Sciences, University of Stavanger, Norway*.

Huang, Z., Wu, T.-R., Tan, S. K., Megawati, K., Shaw, F., Liu, X., & Pan, T.-C. (2009). Tsunami hazard from the subduction Megathrust of the South China Sea: Part II. Hydrodynamic modeling and possible impact on Singapore. *Journal of Asian Earth Sciences, 36*(1), 93-97. doi: http://dx.doi.org/10.1016/j.jseaes.2008.08.007

Kanamori, H. (1983). Magnitude scale and quantification of earthquakes. *Tectonophysics, 93*(3), 185-199.

Kheiri, S., & Bahaari, M. *Evaluation of Ultimate Strength of Jacket Type Structures under Marine Loading.* Paper presented at the Proceedings, 7th International Conference on Coasts, Ports and Marine Structures.

Koh, H. L., Teh, S. Y., Liu, P. L. F., Ismail, A. I. M., & Lee, H. L. (2009). Simulation of Andaman 2004 tsunami for assessing impact on Malaysia. *Journal of Asian Earth Sciences, 36*(1), 74-83.

Kreemer, C., Holt, W. E., Goes, S., & Govers, R. (2000). Active deformation in eastern Indonesia and the Philippines from GPS and seismicity data. *Journal of Geophysical Research: Solid Earth (1978–2012), 105*(B1), 663-680.

Lehfeldt, R., Milbradt, P., Pluss, A., & Schuttrumpf, H. (2007). Propagation of a Tsunami-wave in the North Sea. *Die Kuste*(72), 105-123.

McCalpin, J. (1996). *Paleoseismology* (Vol. 62): Academic press.

Megawati, K., Shaw, F., Sieh, K., Huang, Z., Wu, T.-R., Lin, Y., . . . Pan, T.-C. (2009). Tsunami hazard from the subduction megathrust of the South China Sea: Part I. Source characterization and the resulting tsunami. *Journal of Asian Earth Sciences, 36*(1), 13-20. doi: http://dx.doi.org/10.1016/j.jseaes.2008.11.012

Papazachos, B., Scordilis, E., Panagiotopoulos, D., Papazachos, C., & Karakaisis, G. (2004). Global relations between seismic fault parameters and moment magnitude of earthquakes. *Bull. Geol. Soc. Greece, 36*, 1482-1489.

Pararadarayannis, G. (2001). TSUNAMI HAZARDS.

PTS. (2012). PETRONAS Technical Standard. Design of Fixed Offshore Structures (Working Stress Design). (PTS 34.19.10.30).

Ruangrassamee, A., & Saelem, N. (2009). Effect of tsunamis generated in the Manila Trench on the Gulf of Thailand. *Journal of Asian Earth Sciences, 36*(1), 56-66.

Searer, G. R., & Freeman, S. A. (2004). *Design drift requirements for long-period structures.* Paper presented at the 13th World Conference on.

Appendix I : Joint Displacement for tsunami wave loading of 7m up to 10m

***note : TS01 – 7m, TS02 – 8m, TS03 – 9m, TS04 – 10m**

DATE 10-AUG-2014 TIME 12: 6:36

******* BADP-G BARAM PIPELINE REPLACEMENT PROJECT *********************

JOINT DISPLACEMENTS AND ROTATIONS

LOAD		******** cm	**********	***********	radians	***********	
JOINT	COND	DEFL(X)	DEFL(Y)	DEFL(Z)	ROT(X)	ROT(Y)	ROT(Z)
02	TS04	15.8908	-12.0706	0.8036	0.0047	0.0069	-0.0005
	TS03	10.7949	-8.4585	0.4287	0.0036	0.0050	-0.0004
	TS02	7.8116	-6.2412	0.1994	0.0028	0.0039	-0.0004
	TS01	5.7231	-4.6316	0.0326	0.0022	0.0030	-0.0003
04	TS04	14.6461	-12.1477	-0.9483	0.0047	0.0064	0.0009
	TS03	10.0789	-8.5448	-0.8269	0.0036	0.0047	0.0006

	TS02	7.3547	-6.3264	-0.7336	0.0028	0.0036	0.0004
	TS01	5.4152	-4.7108	-0.6605	0.0022	0.0028	0.0003
06	TS04	15.9698	-10.5520	-0.5650	0.0041	0.0070	-0.0004
	TS03	10.8714	-7.5469	-0.5308	0.0031	0.0051	-0.0003
	TS02	7.8847	-5.6326	-0.5433	0.0025	0.0039	-0.0003
	TS01	5.7922	-4.2014	-0.5690	0.0019	0.0030	-0.0002
08	TS04	14.6232	-10.4987	-1.8997	0.0042	0.0064	0.0012
	TS03	10.0531	-7.4909	-1.5255	0.0033	0.0047	0.0008
	TS02	7.3322	-5.5797	-1.2912	0.0026	0.0036	0.0006
	TS01	5.3994	-4.1544	-1.1196	0.0021	0.0028	0.0005
402	TS04	19.2204	-12.5931	0.6306	-0.0008	0.0008	0.0006
	TS03	13.1582	-8.7900	0.2591	-0.0009	0.0003	0.0004
	TS02	9.6246	-6.4930	0.0371	-0.0008	0.0001	0.0002
	TS01	7.1564	-4.8417	-0.1224	-0.0007	0.0001	0.0001
404	TS04	18.0402	-12.6203	-0.7558	-0.0005	0.0009	0.0003
	TS03	12.4731	-8.8324	-0.7371	-0.0006	0.0005	0.0001
	TS02	9.1805	-6.5436	-0.7080	-0.0006	0.0003	0.0000
	TS01	6.8511	-4.8979	-0.6823	-0.0005	0.0003	0.0000

406	TS04	19.1959	-10.7518	-1.1420	-0.0009	0.0006	0.0011
	TS03	13.1367	-7.6172	-1.0106	-0.0009	0.0002	0.0007
	TS02	9.6025	-5.6655	-0.9595	-0.0009	0.0000	0.0005
	TS01	7.1338	-4.2266	-0.9372	-0.0007	0.0000	0.0004
408	TS04	17.9241	-10.9056	-2.1488	-0.0006	0.0005	0.0009
	TS03	12.3658	-7.7532	-1.7571	-0.0007	0.0001	0.0006
	TS02	9.0842	-5.7927	-1.5184	-0.0006	0.0000	0.0004
	TS01	6.7646	-4.3485	-1.3468	-0.0005	0.0000	0.0003

Appendix II : Member stress report at maximum unity check of 7m up to 10m of tsunami wave height

***note :**

THE FOLLOWING ABBREVIATIONS ARE USED TO DESCRIBE THE CRITICAL UNITY CHECK CONDITIONS:

TN+BN - TENSION PLUS BENDING

BEND - BENDING ONLY (COMP. ALLOWABLES)

C<.15 - COMPRESSION WITH AXIAL LOAD RATIO <.15 (AISC H1-3)

C>.15A - COMPRESSION/BENDING INTERACTION WITH CM'S AND AXIAL LOAD AMPLIFICATION (AISC H1-1)

C>.15B - COMPRESSION/BENDING INTERACTION WITHOUT CM'S AND WITHOUT AXIAL LOAD AMPLIFICATION (AISC H1-2)

SHEAR - EXCEEDS SHEAR ALLOWABLE

L.BEND - CONES: LOCAL BENDING AT CONE - CYL. INTERFACE

HOOP - CONES: HOOP COMPRESSION OR TENSION

EULER - EULER BUCKLIN

DATE 11-AUG-2014 TIME 16: 6:36

******* BADP-G BARAM PIPELINE REPLACEMENT PROJECT **********************

SACS-IV SYSTEM ELEMENT STRESS REPORT AT MAXIMUM UNITY CHECK

MAXIMUM CRITICAL LOAD DIST ********** APPLIED STRESSES ********** * CM VALUES * * NEXT TWO HIGHEST CASES *

MEMBERGRP UNITY COND. CASE FROM AXIAL ** BENDING ** *** SHEAR *** UNITY LOAD UNITY LOAD

CHECK NO. END Y-Y Z-Z Y Z Y Z CHECK COND CHECK COND

m N/mm2 N/mm2 N/mm2 N/mm2 N/mm2

02- 402	PIM	1.152	C>.15B	TS04	0.00	-23.27	-120.94	140.18	9.34	1.16	0.85	0.85	0.86	TS03	0.69	TS02
		0.619	C<.15	TS04	6.90	-26.96	-74.27	85.71	10.95	1.36	0.85	0.85	0.49	TS03	0.40	TS02
04- 404	PIM	1.112	TN+BN	TS04	0.00	23.26	123.99	-127.50	9.03	0.36	0.85	0.85	0.78	TS03	0.58	TS02
		0.582	TN+BN	TS04	6.90	28.08	74.67	-77.19	10.78	0.43	0.85	0.85	0.41	TS03	0.29	TS02
06- 406	PIM	1.350	C>.15B	TS04	0.00	-57.82	-107.75	142.72	8.89	1.79	0.85	0.85	1.02	TS03	0.81	TS02
		0.797	C>.15A	TS04	6.90	-67.82	-66.53	88.83	10.43	2.10	0.85	0.85	0.62	TS03	0.50	TS02
08- 408	PIM	1.052	C<.15	TS04	0.00	-19.47	108.46	-128.98	8.33	1.34	0.85	0.85	0.82	TS03	0.66	TS02
		0.556	C<.15	TS04	6.90	-22.46	67.04	-79.82	9.95	1.58	0.85	0.85	0.45	TS03	0.38	TS02

Appendix III : Member internal load summary for all four legs.

DATE 11-AUG-2014 TIME 16: 6:36

******* BADP-G BARAM PIPELINE REPLACEMENT PROJECT **********************

SACS-IV SYSTEM MEMBER INTERNAL LOADS SUMMARY REPORT

MAX. CRIT LOAD DIST * * * * * * * * * * * I N T E R N A L L O A D S * * * * * * * * * * NEXT TWO HIGHEST CASES

AXIAL SHEAR SHEAR TORSION BENDING BENDING UNITY LD UNITY

LD

CHECK NO. END Y Z Y-Y Z-Z CHECK CN CHECK

CN

m kN kN kN kN-m kN-m kN-m

02- 402 PIM 1.15 C>.15B TS04 0.0 -4129.0 -625.70 542.59 149.18 -7776.8 9014.1 0.9 TS03 0.7 TS02

04- 404 PIM 1.11 TN+BN TS04 0.0 4126.6 575.16 -557.18 46.634 7973.1 -8198.4 0.8 TS03 0.6 TS02

06- 406 PIM 1.35 C>.15B TS04 0.0 -10257. -624.59 481.09 230.51 -6928.6 9177.4 1.0 TS03 0.8 TS02

08-	408	PIM	1.05	C<.15	TS04	0.0	-3454.0	568.02	-473.01	172.70	6974.1	-8293.5	0.8 TS03	0.7	TS02

Appendix IV : Joint Displacement for four legs at operating wave load (OP) and 100 year storm wave load (ST).

***Note : 01 – 0 Degree, 02- 45 Degree, 03- 90 Degree, 04- 135 Degree, 05 – 180 Degree, 06 – 225 Degree, 07 – 270 Degree, 08 – 315 Degree.**

DATE 12-AUG-2014 TIME 16: 6:36

******* BADP-G BARAM PIPELINE REPLACEMENT PROJECT **********************

JOINT DISPLACEMENTS AND ROTATIONS

	LOAD	******** cm	**********	*********** radians	***********		
JOINT	COND	DEFL(X)	DEFL(Y)	DEFL(Z)	ROT(X)	ROT(Y)	ROT(Z)
02	OP01	1.8608	-0.0078	-0.3777	0.0000	0.0011	-0.0002
	OP02	0.4883	0.3327	-0.4420	-0.0002	0.0003	0.0000
	OP03	0.0574	0.2619	-0.4568	-0.0002	0.0001	0.0000
	OP04	-0.5958	0.5208	-0.5025	-0.0004	-0.0003	0.0001
	OP05	-1.1025	-0.0353	-0.4878	0.0000	-0.0006	0.0001
	OP06	-1.1137	-1.0987	-0.4408	0.0006	-0.0006	0.0001
	OP07	0.0859	-1.5382	-0.3549	0.0008	0.0001	0.0000
	OP08	2.0338	-1.7075	-0.2713	0.0009	0.0012	-0.0001
	ST01	4.5069	-0.5510	-0.2528	0.0003	0.0025	-0.0003
	ST02	2.8070	1.2726	-0.3993	-0.0007	0.0017	-0.0002
	ST03	0.3869	1.2786	-0.4869	-0.0008	0.0003	0.0000
	ST04	-0.9887	0.8545	-0.5402	-0.0006	-0.0006	0.0001
	ST05	-1.2210	-0.3252	-0.5061	0.0001	-0.0007	0.0001
	ST06	-1.5332	-2.5137	-0.4047	0.0013	-0.0009	0.0001
	ST07	0.7800	-4.0315	-0.1988	0.0021	0.0005	-0.0001

	ST08	4.1019	-3.3530	-0.0978	0.0017	0.0023	-0.0003
04	OP01	1.8617	-0.0614	-0.4314	0.0001	0.0011	0.0001
	OP02	0.4617	0.3084	-0.4594	-0.0002	0.0003	0.0000
	OP03	0.0158	0.2433	-0.4838	-0.0001	0.0000	0.0000
	OP04	-0.6198	0.5119	-0.4981	-0.0003	-0.0003	0.0000
	OP05	-1.1407	-0.0335	-0.5404	0.0001	-0.0007	-0.0001
	OP06	-1.2111	-1.1058	-0.6077	0.0007	-0.0007	-0.0001
	OP07	-0.0077	-1.5594	-0.5838	0.0009	0.0000	0.0000
	OP08	1.9604	-1.7554	-0.5236	0.0010	0.0012	0.0001
	ST01	4.4675	-0.6260	-0.3826	0.0003	0.0025	0.0003
	ST02	2.7422	1.2300	-0.3280	-0.0007	0.0016	0.0002
	ST03	0.3545	1.2645	-0.4452	-0.0007	0.0002	0.0001
	ST04	-1.0387	0.8465	-0.5275	-0.0005	-0.0006	0.0000
	ST05	-1.3414	-0.3301	-0.5933	0.0002	-0.0008	-0.0001
	ST06	-1.7622	-2.5256	-0.7181	0.0014	-0.0010	-0.0001
	ST07	0.6653	-4.0599	-0.7228	0.0021	0.0004	-0.0001
	ST08	4.0892	-3.4141	-0.5712	0.0017	0.0022	0.0002
06	OP01	1.8996	-0.0002	-0.7091	-0.0001	0.0012	-0.0001
	OP02	0.5237	0.3743	-0.6757	-0.0003	0.0004	0.0000
	OP03	0.0928	0.3241	-0.6507	-0.0002	0.0001	0.0000
	OP04	-0.5604	0.5500	-0.6374	-0.0004	-0.0003	0.0001
	OP05	-1.0604	0.0460	-0.5950	-0.0001	-0.0006	0.0001
	OP06	-1.0655	-0.9202	-0.5413	0.0005	-0.0006	0.0001
	OP07	0.1426	-1.3565	-0.5627	0.0007	0.0001	0.0001
	OP08	2.0858	-1.5678	-0.6383	0.0008	0.0013	-0.0001
	ST01	4.5475	-0.4727	-0.7807	0.0002	0.0026	-0.0003

	ST02	2.8447	1.3560	-0.8241	-0.0008	0.0017	-0.0002
	ST03	0.4141	1.2929	-0.6984	-0.0008	0.0003	-0.0001
	ST04	-0.9486	0.8648	-0.6100	-0.0005	-0.0005	0.0001
	ST05	-1.1623	-0.1464	-0.5679	0.0000	-0.0006	0.0002
	ST06	-1.4682	-2.0944	-0.4690	0.0011	-0.0008	0.0002
	ST07	0.8515	-3.7826	-0.4752	0.0020	0.0005	0.0001
	ST08	4.1639	-3.2944	-0.6202	0.0016	0.0023	-0.0002
08	OP01	1.9032	0.0309	-0.7056	0.0000	0.0012	0.0001
	OP02	0.5101	0.3790	-0.6384	-0.0002	0.0004	0.0000
	OP03	0.0629	0.3231	-0.6216	-0.0001	0.0001	0.0000
	OP04	-0.5668	0.5411	-0.5817	-0.0003	-0.0003	-0.0001
	OP05	-1.0965	0.0217	-0.5889	0.0000	-0.0006	-0.0001
	OP06	-1.1831	-0.9385	-0.6363	0.0006	-0.0007	-0.0001
	OP07	0.0010	-1.3592	-0.7131	0.0008	0.0000	0.0000
	OP08	1.9758	-1.5479	-0.8087	0.0009	0.0012	0.0002
	ST01	4.5005	-0.4273	-0.8388	0.0003	0.0025	0.0003
	ST02	2.8044	1.3851	-0.7053	-0.0007	0.0017	0.0002
	ST03	0.4204	1.3070	-0.6200	-0.0007	0.0003	0.0000
	ST04	-0.9816	0.8608	-0.5576	-0.0005	-0.0006	-0.0001
	ST05	-1.2911	-0.1613	-0.5820	0.0001	-0.0007	-0.0001
	ST06	-1.7459	-2.1108	-0.6669	0.0012	-0.0010	-0.0001
	ST07	0.6548	-3.7754	-0.8891	0.0020	0.0004	0.0001
	ST08	4.0944	-3.2648	-0.9991	0.0017	0.0023	0.0003
402	OP01	2.5539	0.0257	-0.5003	-0.0001	0.0002	-0.0001
	OP02	0.8497	0.4362	-0.5817	-0.0001	0.0002	0.0000
	OP03	0.2875	0.3677	-0.6059	-0.0001	0.0002	0.0000

	OP04	-0.5538	0.6623	-0.6610	0.0000	0.0002	0.0000
	OP05	-1.1706	0.0377	-0.6583	-0.0001	0.0002	0.0000
	OP06	-1.2287	-1.1758	-0.6240	-0.0002	0.0002	0.0000
	OP07	0.3249	-1.6411	-0.5237	-0.0003	0.0002	0.0000
	OP08	2.8023	-1.8636	-0.4103	-0.0003	0.0002	0.0000
	ST01	5.8366	-0.5713	-0.3470	-0.0002	0.0002	-0.0001
	ST02	3.8124	1.5177	-0.4951	-0.0001	0.0003	0.0000
	ST03	0.7181	1.6312	-0.6297	-0.0002	0.0002	0.0001
	ST04	-1.1351	1.1258	-0.7135	-0.0001	0.0001	0.0000
	ST05	-1.4560	-0.2863	-0.6924	-0.0001	0.0002	0.0000
	ST06	-1.8365	-2.7902	-0.6134	-0.0003	0.0001	0.0000
	ST07	1.1847	-4.4195	-0.3878	-0.0005	0.0001	-0.0001
	ST08	5.3560	-3.6228	-0.2344	-0.0005	0.0002	-0.0001
404	OP01	2.5672	-0.0434	-0.5648	0.0001	0.0002	0.0000
	OP02	0.8393	0.3639	-0.6159	0.0001	0.0003	0.0000
	OP03	0.2617	0.2921	-0.6472	0.0001	0.0003	0.0001
	OP04	-0.5598	0.5824	-0.6763	0.0001	0.0002	0.0001
	OP05	-1.1948	-0.0424	-0.7191	0.0001	0.0003	0.0000
	OP06	-1.3189	-1.2626	-0.7802	0.0000	0.0003	0.0000
	OP07	0.2294	-1.7196	-0.7262	-0.0001	0.0003	-0.0001
	OP08	2.7319	-1.9277	-0.6351	-0.0001	0.0003	-0.0001
	ST01	5.8264	-0.6301	-0.4731	0.0000	0.0003	0.0000
	ST02	3.7876	1.4700	-0.4554	0.0001	0.0003	0.0001
	ST03	0.6962	1.5808	-0.6076	0.0001	0.0002	0.0001
	ST04	-1.1677	1.0360	-0.7166	0.0001	0.0001	0.0001
	ST05	-1.5623	-0.3756	-0.7823	0.0000	0.0002	0.0001
	ST06	-2.0433	-2.8893	-0.8911	-0.0001	0.0002	0.0000

	ST07	1.0814	-4.4791	-0.8306	-0.0003	0.0003	-0.0002
	ST08	5.3312	-3.6650	-0.6298	-0.0002	0.0004	-0.0002
406	OP01	2.5291	0.1143	-0.9632	-0.0002	-0.0001	0.0000
	OP02	0.8281	0.5227	-0.9055	-0.0002	0.0000	0.0001
	OP03	0.2651	0.4678	-0.8732	-0.0002	0.0000	0.0001
	OP04	-0.5734	0.7062	-0.8464	-0.0001	0.0000	0.0001
	OP05	-1.1904	0.1220	-0.8015	-0.0002	0.0000	0.0001
	OP06	-1.2552	-0.9725	-0.7558	-0.0003	0.0000	0.0002
	OP07	0.3012	-1.4017	-0.8050	-0.0004	0.0000	0.0002
	OP08	2.7740	-1.6254	-0.9146	-0.0004	0.0000	0.0002
	ST01	5.7949	-0.3636	-1.0799	-0.0002	0.0000	0.0001
	ST02	3.8097	1.7065	-1.0884	-0.0001	0.0001	0.0001
	ST03	0.6860	1.6931	-0.9262	-0.0003	0.0000	0.0000
	ST04	-1.1375	1.1566	-0.8114	-0.0003	-0.0001	0.0001
	ST05	-1.4441	-0.0836	-0.7716	-0.0002	-0.0001	0.0002
	ST06	-1.8576	-2.3392	-0.6858	-0.0003	-0.0001	0.0003
	ST07	1.1710	-4.1066	-0.7572	-0.0005	0.0000	0.0003
	ST08	5.3183	-3.4561	-0.9507	-0.0005	0.0001	0.0002
408	OP01	2.5115	-0.0027	-0.9522	0.0001	0.0000	0.0000
	OP02	0.7896	0.4062	-0.8688	0.0001	0.0001	-0.0001
	OP03	0.2128	0.3546	-0.8430	0.0001	0.0001	-0.0001
	OP04	-0.6053	0.5961	-0.7956	0.0002	0.0000	-0.0001
	OP05	-1.2376	0.0115	-0.7899	0.0001	0.0001	-0.0001
	OP06	-1.3674	-1.0727	-0.8260	0.0000	0.0000	0.0000
	OP07	0.1701	-1.5093	-0.9138	-0.0001	0.0001	0.0001
	OP08	2.6675	-1.7440	-1.0415	-0.0001	0.0000	0.0000

ST01	5.7355	-0.4851	-1.1153	0.0000	0.0001	0.0000
ST02	3.7169	1.5709	-0.9839	0.0001	0.0001	0.0000
ST03	0.6550	1.5974	-0.8523	0.0001	0.0000	-0.0001
ST04	-1.2175	1.0580	-0.7594	0.0001	-0.0001	-0.0001
ST05	-1.5829	-0.1913	-0.7745	0.0001	-0.0001	-0.0001
ST06	-2.0875	-2.4181	-0.8344	0.0000	0.0000	0.0001
ST07	0.9923	-4.1935	-1.0758	-0.0002	0.0000	0.0002
ST08	5.2684	-3.5852	-1.2387	-0.0002	0.0001	0.0000